IC/SMR/204 - 32

WINTER COLLEGE ON

ATOMIC AND MOLECULAR PHYSICS

(9 March - 3 April 1987)

Background material on Laser Chemistry
and Diagnostic of Combustion Processes using
Excimer- and Dye-Laser Systems

J. Wolfrum
Physikalisch-Chemisches Institut
Heidelberg
West Germany

Einsatz von Excimer- und Farbstofflasern zur Analyse von Verbrennungsprozessen

Diagnostic of Combustion Processes using Excimer- and Dye-Laser Systems

J. Wolfrum

Zusammenfassung

Durch die Entwicklung leistungsfähiger Laserlichtquellen im sichtbaren und UV-Bereich sind auf dem Gebiet der berührungsfreien Diagnostik von Verbrennungs- und Strömungsvorgängen wesentliche Fortschritte erzielt worden. Durch Einsatz linearer und nichtlinearer laserspektroskopischer Techniken (LIF, CARS, REMPI, RAMAN-, RAYLEIGH- und MIE-Streuung) können Konzentrationen und Temperaturen mit hoher zeitlicher Auflösung sowohl punktweise wie auch zweidimensional erfaßt werden.

1. EINLEITUNG

Die komplexe Wechselwirkung zwischen einer großen Zahl von chemischen Elementarreaktionen und Strömungs- sowie Transportvorgängen bestimmt den Ablauf technisch genutzter Verbrennungsprozesse. Ein grundlegendes Verständnis dieser Wechselwirkung ist notwendig, wenn in Zukunft entscheidende Fortschritte bei einer besseren Ausnutzung der Kraftstoffe und einer Verminderung der Bildung von Schadstoffen erzielt werden sollen /1/. Interessante neue Möglichkeiten bietet hier die mathematische Simulation auf modernen Großrechenanlagen. Eine Aufstellung realistischer Simulationsmodelle ist aber nur möglich, wenn es gelingt, mit Hilfe einer berührungsfreien Diagnostik Informationen über Temperatur, Konzentrationen und Geschwindigkeiten der reagierenden Teilchen mit hoher räumlicher und zeitlicher Auflösung zu erhalten. Durch die Entwicklung leistungsfähiger Laserlichtquellen wie z.B. Excimer- und Farbstofflaser im sichtbaren und UV-Bereich sind auf dem Gebiet der berührungsfreien Diagnostik wesentliche Fortschritte erzielt worden. Im nachfolgenden Beitrag soll der Einsatz derartiger linearer und nicht-linearer laserspektroskopischer

Techniken, wie laserinduzierte Fluoreszenz (LIF), Resonante Mehrphotonenionisation (REMPI), Kohärente Anti-stokes-Raman-Spektroskopie (CARS) - sowie Raman-, Rayleigh- und Mie-Streuung zur Analyse von Verbrennungsprozessen beschrieben werden.

2. LASERINDUZIERTE FLUORESZENZ (LIF)

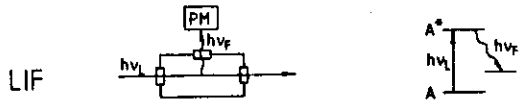

Abb. 1 Prinzip der LIF-Spektroskopie

Wie in Abb. 1 schematisch gezeigt, wird beim LIF-Verfahren abstimmbares Laserlicht zur selektiven Anregung eines elektronischen Übergangs in einem Atom oder Molekül benutzt. Nach der Anregung des Teilchens kann entweder die gesamte Fluoreszenz als Funktion der eingestrahlten Laserwellenlänge (Anregungsspektrum) oder die spektralaufgelöste Fluoreszenz (Fluoreszenzspektrum) zur Bestimmung von Teilchenkonzentration und Temperatur benutzt werden. LIF zeichnet sich durch eine sehr hohe Empfindlichkeit und Spezifität im Nachweis aus, ist jedoch an geeignete elektronische Übergänge der nachzuweisenden Teilchen gebunden. Ein wesentliches Problem bei der quantitativen Auswertung von LIF-Signalen aus Verbrennungsprozessen ist die Löschung ("quenching") der angeregten Elektronenzustände durch desaktivierende Stöße innerhalb ihrer Strahlungslebensdauer. Diese Löschprozesse können zwar in getrennten Experimenten untersucht werden[2], sind aber wesentlich von der lokalen Zusammensetzung und Temperatur der Flammengase abhängig und damit schwer quantitativ zu berücksichtigen. Erreicht man durch eine sehr hohe Laserintensität eine Gleichbesetzung der Zustände A und A* (s. Abb. 1) ("gesättigte Fluoreszenz"), so spielt die durch Stöße reduzierte Strahlungslebensdauer keine Rolle mehr und man erhält einen einfachen Zusammenhang

zwischen Fluoreszenzintensität und Teilchenkonzentration[3]. Der gesättigte Zustand ist jedoch ein Grenzfall, der im Experiment nicht völlig erreichbar ist, da innerhalb des Laserimpulses räumlich und zeitlich stets Randzonen mit geringerer Intensität vorhanden sind, doch kann der Grad der Sättigung über Messungen der Fluoreszenzlichtverteilung in zwei zueinander senkrechten Richtungen im Laserstrahl bestimmt werden[4]. Eine weitere Möglichkeit der quantitativen Auswertung von LIF-Signalen ist die gleichzeitige Anwendung von LIF und Absorptionsmessungen[5, 6]. Der Einsatz von LIF zur Diagnostik von reaktiven Strömungen wird besonders interessant durch die Möglichkeit, neben Einzelpunktmessungen auch Informationen simultan in mehreren Dimensionen erhalten zu können, wie sie zur quantitativen Modellierung turbulenter Verbrennungsvorgänge unbedingt notwendig sind.

Nachweis von Radikalen

Durch LIF können zahlreiche freie Atome und Radikale (wie z. B. H, O, N, C, OH, CH, CN, C_2, NH, NH_2, HNO, SH, SO, S_2, CS, NCO, C_3, CH_3O u.a.) nachgewiesen werden, die in Verbrennungsprozessen als rasch reagierende Zwischenprodukte auftreten.

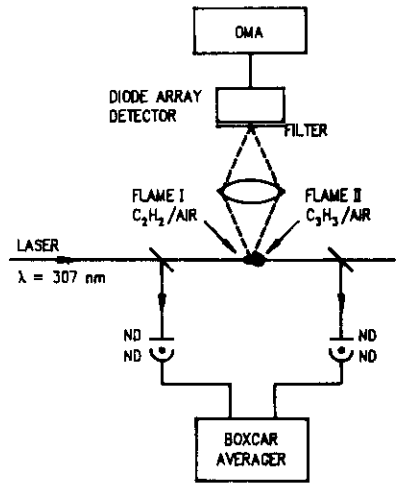

Abb. 2 zeigt schematisch eine experimentelle Anordnung zum Nachweis von OH-Radikalen, mit Hilfe der kombinierten LIF- Absorptionsspektroskopie. Hierdurch lassen sich OH-Konzentrationsprofile senkrecht zur Flammenausbreitungsrichtung bestimmen[6].

Durch Einsatz einer Oszillator-Verstärker-Kombination für einen XeCl-Excimer-Laser erhält man eine schmalbandig abstimmbare Emission im Bereich von 308 nm, die eine effektive Anregung der OH-Radikalfluoreszenz erlaubt. Die Pulsenergie eines derartigen Lasersystems liegt mehr als zwei Größenordnungen über den Leistungen, die sich aus Frequenzverdopplung von Farbstofflasern in diesem Wellenlängenbereich erzielen lassen, so daß eine Anregung der gesättigten Fluoreszenz von OH-Radikalen auch bei hohen Drucken, wie sie bei der motorischen Verbrennung auftreten, möglich ist. Durch Einsatz eines zweidimensionalen Dioden-Array-Detektors in Kombination mit einem Bildverstärker[8], empfindlicher Vidiconkameras[9] und CCD (Charge-Coupled-Device) Arrays[10] kann die durch den "Laser-Lichtschnitt" erhaltene Verteilung der Radikalkonzentrationen elektronisch gespeichert und ausgewertet werden.

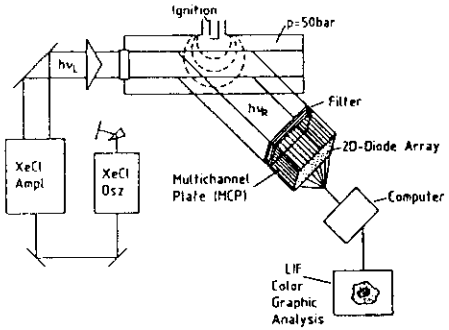

Abb. 3 2-dimensionale Darstellung der OH-Radikalkonzentrationen im Verbrennungsmotor durch Laser-Lichtschnitt LIF-Spektroskopie

Ähnlich wie OH lassen sich auch CH-Radikale, die ein Indikator für die Ausdehnung und momentane Lage der Flammenfront sind, über zweidimensionale LIF nachweisen. Die Anregung erfolgt dabei in der CH-Bande bei 426 nm und der Nachweis bei 431,5 nm mit Hilfe eines 3-stufigen Filters von 1 nm Halbwertsbreite[11]. Die hierbei notwendige scharfe spektrale Trennung zwischen Laserstreulicht und Fluoreszenzlicht kann umgangen werden, wenn, wie in Abb. 4 schematisch gezeigt, zur Anregung Mehrphotonenprozesse benutzt werden[12].

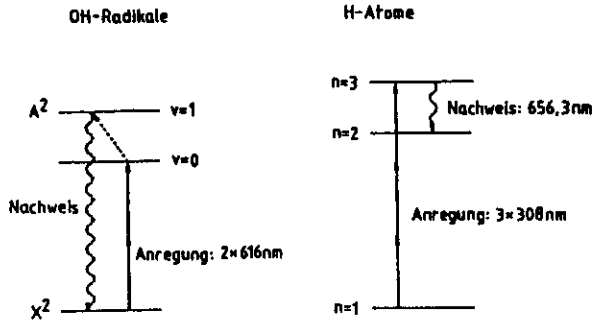

Abb. 4 Nachweis von H-Atomen und OH-Radikalen durch Mehrphotonen-LIF-Spektroskopie

Auf diese Weise lassen sich auch Zustände, deren Einphotonenabsorptionen im UV oder Vakuum-UV liegen, in Flammen anregen und über eine wesentlich längerwellige LIF-Emission beobachten, so z.B. Sauerstoffatome mit der Emission bei 778 nm und Wasserstoffatome über die Balmer-α-Linie bei 656 nm[12,13]. Durch Einsatz von ArF-Excimer-Laserstrahlung bei 193 nm lassen sich im Verbrennungsprozeß intermediär gebildete Produkte, wie z.B. C_2H_2, durch einen 2-Photonen-Prozeß dissoziieren, wobei im Fragment CH die Emission $A \longrightarrow X$ bei 431 nm beobachtet wird[11].

Nachweis von stabilen Molekülen

Durch Zusatz bestimmter fluoreszierender Moleküle zum Brennstoff, wie z.B. NO_2[14], NO[15], CO[16], können durch zweidimensionale LIF-Spektroskopie Informationen über Temperaturen und Gebiete mit und ohne Brennstoff und damit über die momentane Lage der Flammenfronten gewonnen werden. Allerdings lassen sich auf diese Weise meist nur qualitative Daten gewinnen, da die Fluoreszenz der genannten Teilchen durch Stöße gelöscht werden kann. Dieses Problem kann man umgehen, wenn Teilchen zur Fluoreszenz in elektronischen Zuständen angeregt werden, deren Lebensdauern infolge von Prädissoziationen oder interner Energieumwandlung sehr viel kürzer als die Stoßzeiten sind. Wie in Abb. 5 schematisch gezeigt, gelingt dies für O_2[17] durch

Anregung mit einem ArF-Excimer-Laser bei 193 nm. Eine Reihe aromatischer Kohlenwasserstoffe sowie Aldehyde können bereits durch Anregung mit XeCl-Excimerlaser bei 308 nm in Zustände mit sehr kurzer Lebensdauer angeregt werden. Für Acetdaldehyd (CH_3HCO) konnte gezeigt werden, daß bis zu Drucken von 25 bar keine wesentliche Änderung der Fluoreszenzquantenausbeute eintritt[19].

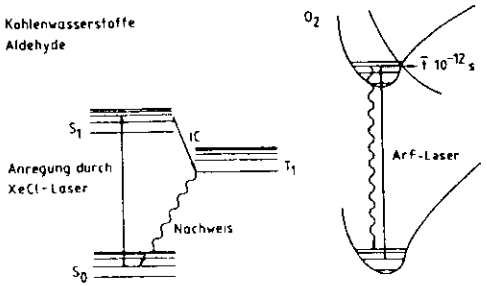

Abb. 5 LIF-Nachweis von Molekülen mit kurzer Strahlungslebensdauer

Nachweis von Flüssigkeits/Dampf Mischungen

Ein interessante Anwendung der LIF-Technik ist die Untersuchung der Verdampfung von Tröpfchen wie etwa im Zusammenhang mit der Gemischbildung bei Dieselkraftstoff. Durch Zusatz bestimmter organischer Moleküle, die in der Lage sind, Komplexe in einem elektronisch angeregten Zustand ("Exciplex" = Excited State Complex) zu bilden, kann der Übergang zwischen flüssiger und gasförmiger Phase anhand der Verschiebung der Fluoreszenzwellenlänge verfolgt werden. Die in einer reversiblen Reaktion gebildeten Exciplexe finden sich vorwiegend in der flüssigen Phase. In der Gasphase dominiert die Emission des freien Monomers. Beide Emissionen können bis zu 150 nm spektral verschoben sein[20]. In ersten Experimenten wurde die frequenzvervierfachter Strahlung eines Nd-YAG-Lasers bei 266 nm zur Anregung benutzt und die Fluoreszenz mit Hilfe eines fotografischen Films registriert [21, 22]. Der Einsatz von Excimerlasern und zweidimen-

sionalen Dioden-Array Kameras sollte Einzelimpulsdarstellungen erlauben. Ein Problem ist die starke Löschung der Fluoreszenz in der Gasphase durch Sauerstoff. Dies ist beim Nachweis der Tröpfchen kein Problem, da Sauerstoff nur langsam in die Flüssigkeit hinein deffundiert. Es erscheint möglich, mit Hilfe der Fluoreszenztechnik auch Informationen über die Tröpfchentemperaturen zu erhalten[22, 23]. Setzt man der zu zerstäubenden Flüssigkeit einen Farbstoff zu, der bei Anregung mit Licht relativ schwach absorbiert, so kann man aus der Intensitätsverteilung im Laserlichtschnitt Informationen über die Verteilung und Größe der Tröpfchen erhalten[24].

Bestimmung von Temperaturfeldern

Die selektive Anregung molekularer Zustände mit Hilfe der LIF erlaubt eine Bestimmung relativer Besetzungsgrade und damit Rückschlüsse auf die lokalen Temperaturen. Regt man mit Lasern unterschiedlicher Wellenlänge OH-Radikale aus verschiedenen Schwingungszuständen des elektronischen Grundzustands in das gleiche Rotationsschwingunsniveau des angeregten Elektronenzustands an, so kann aus dem Verhältnis der beiden Emissionsintensitäten die Temperatur direkt ermittelt werden. Löschprozesse stören dabei nicht, da die Emission aus dem gleichen oberen Zustand erfolgt[25].

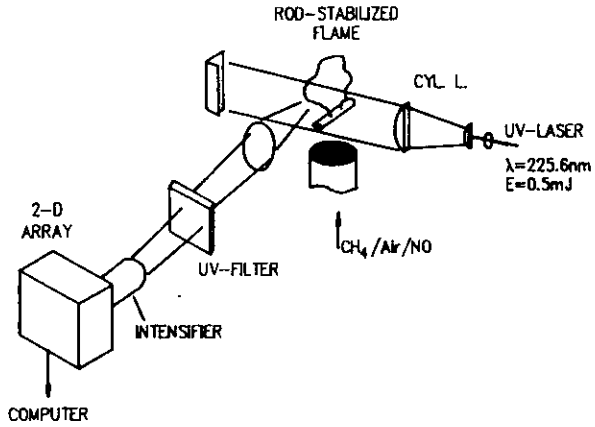

Abb. 6 Messung von Temperaturverteilungen in Methanflammen durch LIF-Spektroskopie an zugesetzten NO-Molekülen[15]

Ein Nachteil dieses Verfahrens ist, das nur Temperaturen erfasst werden können, wenn die Gleichgewichtskonzentration an OH-Radikalen für einen LIF-Nachweis ausreicht. Eine Alternative ist der Zusatz eines geeigneten molekularen "Tracers" zur Temperaturmessung, wie z.B. das thermisch sehr stabile Molekül NO. Wie in Abb. 6 gezeigt, kann durch Anregung bei NO bei 225,6 nm das Temperaturfeld einer Methan-Flamme vermessen werden. Die bisher erzielten Ergebnisse sollten sich durch Einsatz leistungsstarker Excimerlaser verbessern lassen /26/.

3. SPONTANTE RAMANSTREUUNG

Spontane Ramanspektroskopie von Verbrennungsprozessen wird seit Aufkommen der Lasertechnik intensiv betrieben /27, 28/. Durch Einsatz von abstimmbaren Excimerlasern können im Einzelschuß vollständige Ramanspektren aufgenommen werden.

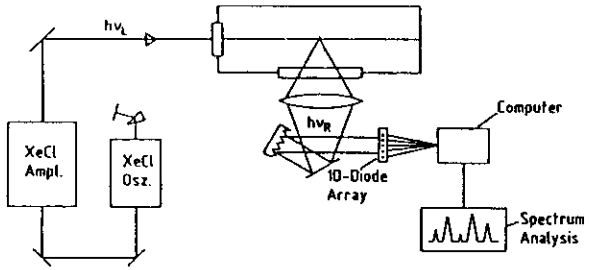

Abb. 7 Aufnahme von spontanen Ramanspektren im Einzelimpulsbetrieb durch Anregung mit einem abstimmbaren Excimerlaser.

Der Nachweis von n-Heptan und Stickstoff durch spontane Ramanstreuung erlaubt die Gemischbildung bei den Dieseleinspritzungen punktweise direkt zu verfolgen. In turbulenten Diffusionsflammen können in Einzelmessungen simultan mehrere Teilchenkonzentrationen (N_2, CO_2, O_2, CO, CH_4, H_2O, H_2) sowie Temperaturen ermittelt werden /30/. Dabei wird ein intensiver Farbstofflaser mit relativ langer Pulsdauer benutzt. Auch eine zweidimensionale Darstellung der Verteilung von Methan in einer turbulenten, nichtvorgemischten Methan-Wasserstoff-Luftflamme ist möglich /31/. Es wurde ein Laserpuls von 200 mJ Energie

bei 440 nm und 1,8 µsec Dauer mehrfach in der in Abb. 11 gezeigten Weise durch die Flamme geführt. Da der gesamte Q-Zweig der Ramanemission des CH_4 aufgenommen wurde, sind die erhaltenen Signale proportional zur CH_4 Konzentration. Eine automatische Kalibrierung erfolgte durch die Aufnahme der einströmenden Flammengase.

4. CARS-SPEKTROSKOPIE

CARS (Kohärente Anti-Stokes-Ramanspektroskopie) erlaubt die Messung von Temperatur und Konzentrationen ramanaktiver Spezies mit hoher zeitlicher, räumlicher und spektraler Auflösung.

Abb. 8 Prinzip der CARS-Spektroskopie

Wie in Abb. 8 gezeigt beobachtet man CARS-Signale, wenn zwei Laserstrahlen, Pump- und Stokesstrahl, mit Frequenzen ω_p und ω_s ($\omega_p > \omega_s$) über die dielektrische Suszeptibilität 3. Ordnung $\chi^{(3)}$ des Mediums wechselwirken. Die Signalintensität bei der Frequenz $\omega_{CARS} = 2\omega_p - \omega_s$ hängt dabei einerseits quadratisch von der Intensität des Pumplasers und andererseits vom Betragsquadrat der oben erwähnter dielektrischer Suszeptibilität ab.

$$I_{CARS} \sim I_p^2 I_s /\chi^{(3)}/^2$$

Die Intensität des CARS-Signals steigt resonanzartig an, sobald $\omega_p - \omega_s$ der Frequenz eines Ramanübergangs ω_J des Mediums entspricht. Bei festgehaltener Pumplaserfrequenz lassen sich durch Veränderung der Stokes-Laserfrequenz verschiedene Rotations-Schwingungsübergänge eines Moleküls abtasten. Temperatur und Konzentration werden durch Berechnung der dielektrischen Suszeptibilität dritter Ordnung ermittelt. Die komplexe dielektrische Suszeptiblität eines beobachteten Übergangs hängt u.a. von der Besetzungszahldifferenz der

beteiligten Molekülzustände ab[33]. Zusätzlich tritt ein durch den nichtresonanten Term χ_{NR} verursachter spektral glatter Hintergrund des CARS-Signals auf. Werden die beiden Laserstrahlen kollinear überlagert, so erhält man eine räumliche Auflösung von 50 - 100 µm senkrecht und 1 - 3 cm parallel zur Strahlrichtung. Durch spezielle Strahlanordnungen (USED-CARS, BOXCARS) sind longitudinale Auflösungen bis in den sub-Millimeterbereich möglich[34, 41].

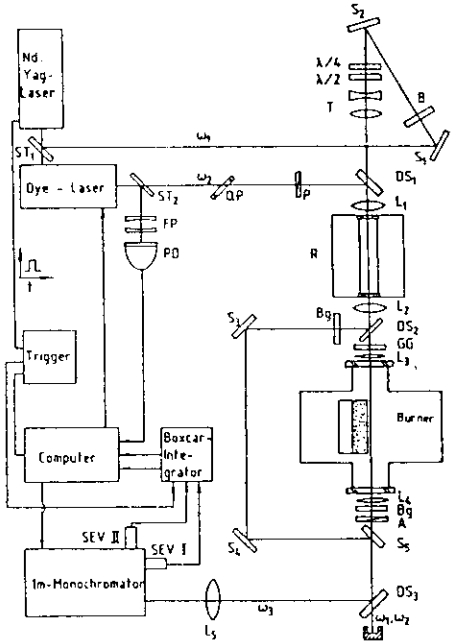

Abb. 9 Schema einer CARS Anordnung zur Untersuchung laminarer Gegenstrom-Diffusionsflammen[35]

Bei der USED (Unstable Resonator Spatially Enhanced Doughnutbeam)-CARS-Konfiguration wird der Stokes-Strahl innerhalb des ringförmigen Pumplaserstrahls justiert[41]. Wie in Abb. 9 gezeigt, werden zunächst Pump- und Stokeslaserstrahl innerhalb einer mit Argon gefüllten Zelle räumlich überlappt. Nach Rekollimierung und erneuter Fokussierung wird im Meßbereich einer Methan/Luft Gegenstrom Diffusionsflamme das CARS-Signal des spektroskopierten Moleküls erzeugt. Referenzsignal und CARS-Signal werden nach Durchgang durch einen Monochromator räumlich separiert, durch zwei Photomultiplier detektiert und durch einen Rechner weiter verarbeitet[35]. Die Auswertung der Spektren

erfolgt durch Anpassen von $\chi^{(3)}$ an das gemessene Spektrum. Als Parameter werden Temperatur und Konzentration des berechneten Spektrums bis zur bestmöglichen Übereinstimmung variiert.

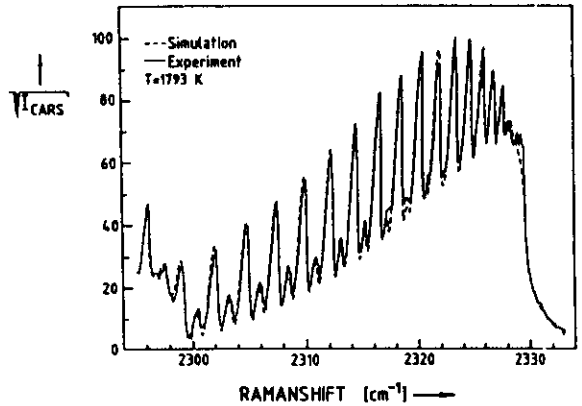

Abb. 10 N_2-CARS-Spektum gemessen in einer Methan/Luft Gegenstrom-Diffusionsflamme bei Atmosphärendruck[35]

Die Berechnung der Ramanfrequenzen des Übergangs und der Besetzungszahldifferenz aufgrund bekannter spektroskopischer Daten ist für zweiatomige Moleküle in einigen Fällen mit hoher Genauigkeit möglich. Mit CARS-Spektroskopie an N_2 konnten hierdurch Gastemperaturen mit einer Genauigkeit von 40 K bei 2000 K gemessen werden[36]. Die gegenwärtigen Forschungsarbeiten konzentrieren sich auf die Berücksichtigung der Modenstruktur der verwendeten Laser[37] und Modelle, die auch Stoßwechselwirkungen der Moleküle berücksichtigen[38]. Wird der nichtresonante Hintergrund der dielektrischen Suszeptibilität durch Polarisationstechniken unterdrückt, so können durch statistische Fluktuationen der Modenstruktur verursachte Effekte vernachlässigt werden[39]. Zentrales Problem bei der Berücksichtigung der Stoßwechselwirkung der Moleküle ist die korrekte Berechnung der Linienbreiten der Ramanübergänge. Für den Druckbereich 0,2 - 2 atm (der Bereich des "collisional broadening") liegt ein analytischer Ausdruck

für die Halbwertsbreite der Ramanübergänge in Abhängigkeit von Temperatur, Rotationsquantenzahl des Übergangs und Druck des Mediums vor[40]. Bei höherem Druck tritt "collisional narrowing" auf - eine Einengung des CARS-Spektrums um das bei der betreffenden Temperatur am stärksten besetzte Rotationsniveau[41]. CARS-Spektroskopie in Hochdrucksystemen - wie etwa Verbrennungsmotoren (s. Abb. 11) - erfordert eine Simulation der Spektren unter Berücksichtigung des "collisional narrowing"[42, 43].

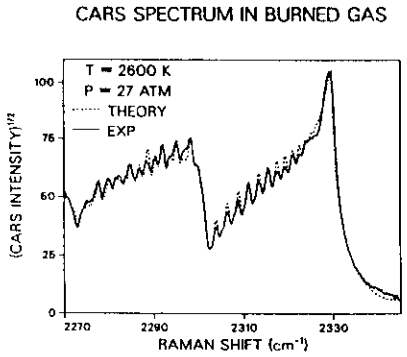

Abb. 11 N_2-CARS Spektrum gemessen im Brennraum eines Otto-Motors[43]

Bei der Rotations-CARS-Spektroskopie erhält man höhere Anregungsquerschnitte, die auf Grund der sich stark ändernden Besetzungen der Rotationslinien jedoch nur bei Temperaturen unter 1000 K Vorteile bringen[44, 45]. Bei Benutzung einer Multiplexanordnung mit Hilfe von Breitband-Farbstofflasern ist eine Kombination von Schwingungs- und Rotations-CARS möglich, dies erlaubt eine Temperaturmessung zusammen mit einer Mehrkomponenten-Konzentrationsanalyse mit nur einem Laserimpuls[45, 46].

5. RAYLEIGH UND MIE-STREUUNG

Gegenüber der unelastischen Wechselwirkung von Photonen mit Molekülen, wie sie bei der Raman-Streuung beobachtet wird, erhält man bei

der elastischen Streuung an Molekülen (Rayleigh-Streuung) wesentlich größere Streuquerschnitte, die allerdings immer noch deutlich unter denen für LIF liegen. Da die Rayleigh-Streuung keine Wellenlängenverschiebung zeigt, kann sie nur angewendet werden, wenn keine Partikel oder Oberflächen in den untersuchten Prozessen zu störendem Streulicht führen. Abb. 12 zeigt Methan-Wasserstoff-Luftflamme, deren Temperaturfeld mit Hilfe der Rayleigh-Streuung vermessen wurde. Die Brenngaszusammensetzung wurde dabei so gewählt, daß Brenngas, die umgebende Luft und die Verbrennungsprodukte in ihrem Rayleighstreuquerschnitt nur sehr geringe Unterschiede zeigen. Es wurde ein Farbstofflaser bei 440 nm mit 200 mJ Pulsenergie benutzt. Der Einsatz von Excimerlasern mit kürzeren Wellenlängen sollte auf Grund der Abhängigkeit des Rayleigh-Signals von der reziproken 4. Potenz der Laserwellenlänge weitere Verbeserungen in der Signalintensität ermöglichen.

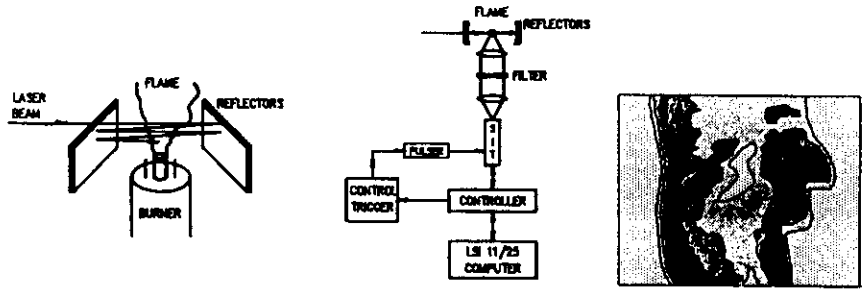

Abb. 12 Messung der planaren Temperaturverteilung in einer turbulenten CH_4-H_2-Luft-Flamme durch Rayleighstreuung[31]

Benutzt man als Streuzentren makroskopische Partikel, so erhält man eine weitere Steigerung der Streuintensität, so daß zum Nachweis fotografischer Film und unverstärkte Dioden-Array Kameras benutzt werden können. Bei der Aufzeichnung durch Film erhält man eine hohe Auflösung, während die Realzeitdarstellung und die direkte Rechner-

auswertung bei Dioden-Array Kameras von Vorteil sind. Die Anwendung der Mie-Streuung zur Charakterisierung von Verbrennungsprozessen ist möglich, wenn den Verbrennungsgasen geeignete Substanzen zugesetzt werden, bei denen es in der Flammenfront zu einer Partikelbildung kommt. Eine interessante Möglichkeit ist in Abb. 13 gezeigt[47]. Durch Zusatz von $TiCl_4$ bilden sich bei Kontakt mit den in der Flammenfront entstandenen Wassermolekülen TiO_2 Partikel im Sub-Mikronbereich, die als Streuzentren dienen. Durch diese Mie-Streumessungen wurde gezeigt, das die Flammenfronten sehr dünn sind (100 - 300 µm) und mit steigender Motordrehzahl von schwach gekrümmten kontinuierlichen Fronten in stärker gewinkelte übergehen, sowie Bereiche mit unverbranntem Gas stärker in Erscheinung treten (s. Abb. 13). Die Technik der TiO_2 Teilchenbildung kann auch zur Sichtbarmachung von Mischvorgängen benutzt werden, wobei ein wasserfreier Gasstrom mit $TiCl_4$ versetzt wird und dem zweiten Gasstrom Wasserdampf zugesetzt ist[48]. Unter bestimmten Bedingungen können auch Rußteilchen, die sich während der Verbrennung bilden, zum Nachweis von Flammen durch Mie-Streuung benutzt werden[49].

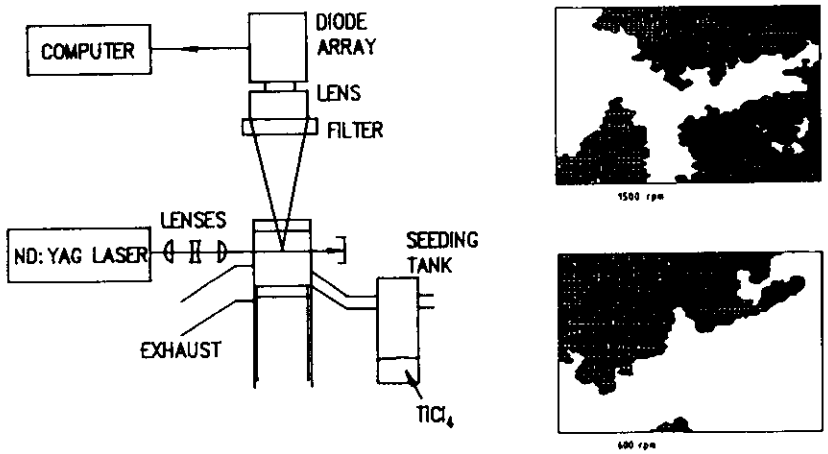

Abb. 13 Zweidimensionale Darstellung der momentanen Lage der Flammenfronten in einem Verbrennungsmotor durch Laser-Mie-Streuung an TiO_2-Partikeln[47].

6. RESONANTE MEHRPHOTONENIONISATION (REMPI)

Die Möglichkeit eines extrem empfindlichen Nachweises einzelner Moleküle bietet die resonante Mehrphotonenionisation (REMPI). Wie in Abb. 14 am Beispiel des Schadstoffes NO gezeigt, wird dabei mit Hilfe eines Ein- oder Zweiphotonenprozesses zunächst ein resonanter Zwischenzustand besetzt, von dem die selektive Ionisierung mit einem weiteren Laserphoton erfolgt. Durch Einführung einer Mikroprobe zum Nachweis der gebildeten Ionen können auf diese Weise in Flammen NO[50], CO[51], CH_3-Radikale[52], Sr[53], PO[54], Li[55], Th und Pb[56], H- und O-Atome[57] und andere Teilchen nachgewiesen werden.

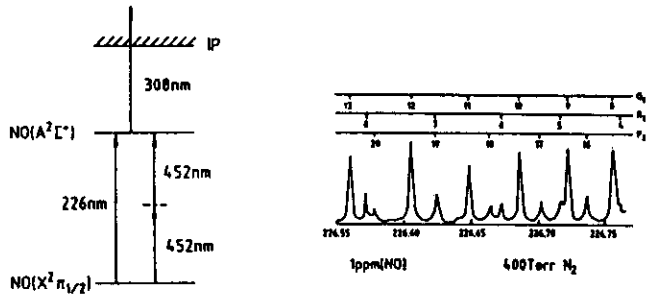

Abb. 14 Nachweis von NO durch REMPI Spektroskopie

7. AUSBLICK

Das Gebiet der Diagnostik von Verbrennungsvorgängen mit Hilfe leistungsstarker UV-Laser befindet sich in einer raschen Entwicklung. Excimerlaser mit einer Wiederholfrequenz im Bereich von kHz werden in nächster Zukunft zur Verfügung stehen. Metalldampflaser erlauben mit geringeren Pulsenergien Wiederholraten bis zu 20 kHz. Für den Nachweis zweidimensionaler Laserlichtschnitte sind CCD-Arrays mit hoher Auflösung (10^6 Pixel) bereits erhältlich. Durch diese Technik wird es auch möglich, dreidimensionale Abbildungen von Temperatur und Teilchenkonzentration zu erstellen, die wesentliche Anstöße für die realistische Modellierung von Verbrennungsprozessen unter extremen Bedingungen geben werden.

8. Literatur

/1/ 1. TECFLAM-SEMINAR Heidelberg, Schadstoffe bei Verbrennungsvorgängen (Stuttgart 1985)

/2/ Jeffries, J.B., Copeland, R.A., Crosley, D.R., J. Chem. Phys. 85, 1898 (1986)

/3/ Daily, J.W., Appl. Opt. 16, 568 (1977)
Kohse-Höinghaus, K., Heidenreich, R., Just, Th., 20th Symp. (Int.) on Combustion, p. 1177, Pittsburgh (1985)

/4/ Cottereau, M. J., Opt. Lett (1986)

/5/ Stepowski, D., Garo, A., Appl. Opt. 24, 2478 (1985)

/6/ Hertz, H. M., Alden, M., Proc. CLEO, p. 362, San Francisco (1986)

/7/ Alden, M., Edner, H., Holmsted, G., Svanberg,S., Högberg, T., Appl. Opt. 21, 1236 (1982)

/8/ Kychakoff, G., Howe, R.D., Hanson, R.K., Appl. Opt. 23, 704 (1984)

/9/ Cattolica, R.J.,Vosen, S.R., 20th Symp. (Int.) on Combustion, p. 1273, Pittsburgh (1985)

/10/ Paul, P., Kychakoff, G., Hanson, R.K., Appl. Opt. (1986)

/11/ Allen, M.G., Hanson, R.K., 21st Symp. (Int.) on Combustion, Pittsburgh (1987)

/12/ Goldsmith, J.E.M., Anderson, R.J.M., Appl.Opt.24, 607(1985)
Goldsmith, J.E.M., Laurendeau, N.M., Appl.Opt.25, 276(1986)

/13/ Alden, M., Wallin, S., Wendt, W., Appl. Phys. B33, 205 (1984)

/14/ Cattolica, R.J., Vosen, S.R., Comb. and Flame (1986)

/15/ Seitzman, J.M., Kychakoff, G., Hanson, R.K., Opt. Lett. 10, 439 (1985)

/16/ Haumann, J., Seitzman, J.M., Hanson, R.K., Opt. Lett. 11 (1986)

/17/ Massey, G.A., Lemon, C.J.,IEEE J. Quant. Elec. QE-20, 454 (1984)

/18/ Itoh, F., Kychakoff, G., Hanson, R.K.,J. Vac. Sci. Technol. B3(6), 1600 (1985)

/19/ Kleinermanns, K., Monkhouse, P., Suntz, R., Wolfrum, J., Chem.Phys. Lett. (1986)

/20/ Melton, L.A., Appl. Opt. 22, 2224 (1983)

/21/ Melton, L.A., Verdieck, J.F.,20th Symp.(Inter.)on Combustion, p. 1238, Pittsburgh (1985)

/22/ Melton, L.A., Verdieck, J.F.,
Comb.Sci. and Tech. 42, 217 (1985)

/23/ Murray, A.M., Melton, L.A., Appl.Opt. 24, 2783 (1985)

/24/ Brown, G.M., Kent, J.C. in Flow Visualization III (Ed. W.J. Yang), p. 118, Hemisphere Pub.Corp. (1985)

/25/ Cattolica, R.J., Stephenson, D.A., in Progress in Astronautics and Aeronautics 95, 714(1985)

/26/ Lee, M.P., Paul, P.H., Hanson, R.K.,Opt.Lett.11 (1986)

/27/ Hartley, D.L in Laser Raman Gas Diagnostics (Eds. M. Lapp and C.M. Penney) p. 311, Plenum (1974)

/28/ Knoche, K.F., Daams, H.-J., Bahnen, R., Hassel, E., VDI-Berichte 498, 215 (1983)

/29/ Pischinger, F., Scheid, E., Knoche, K.F., Daams, H.-J., Heinze, T. Reute, U., SAE Paper No. 861121 (1986)

/30/ Dibble, R.W., Masri, A.R., Bilger, R.W., Combustion and Flame (1986)

/31/ Long, M.B., Levin, P.S., Fourguette, D.C., Opt.Lett.10, 267 (1985)

/32/ Péalet, M., Taran, J.P., Taillet, J., Bacal, M., Bruneteau, A.M., Combust. Flame 54, 149 (1983)

/33/ Tolles, W.M., Nibler, J.W., McDonald, J.R., Harvey, A.B., Appl. Spectroscopy 31 253 (1977)

/34/ Druet, S.A.J., Taran, J.P., CARS-Spectr., Office National D'Etudes et de Recherches Aérospatiales, Chatillon,

/35/ Dreier, T., Lange, B., Wolfrum, J., Zahn, M., Behrendt, F., Ber.Bunsenges.phys.Chem (1986)

/36/ Péalet, M., Taran, J.P., Taillet, J., Bacal, M., Bruneteau, A.M., J.Appl. Phys. 52, 2687 (1981)

/37/ Teets, R.E., Opt. Lett. 9, 226 (1984)

/38/ Sala, J.P., Bonamy, J., Robert, D., Lavorel, B., Millot, G., Berger, H., Chem. Phys. 106, 427 (1986)

/39/ Farrow, R.L., Rahn, L.A., F.Opt.Soc.Am. B2, 903 (1985)

/40/ Hall, R.J., Appl. Spectrosc. 34, 700 (1980)

/41/ Hall, R., Eckbreth, A., in Laser Applications, (Eds. J.F. Ready R.K. Erf), Academy Press, Orlando (USA)

/42/ Farrow, R.L., Lucht, R.P., Clark, G.L., Palmer, R.E., Appl. Opt. 24, 2241 (1985)

/43/ Green, R.M., Lucht, R.P., Proc. Int. Symp. on Diagnostics and Modeling of Combustion in Reciprocating Engines, Tokyo (1985)

/44/ Zheng, J.B., Snow, J.B., Murphy, D.V., Leipertz, A., Chang, R.K., Farrow, R.L., Opt. Lett. 9, 341, (1984)

/45/ Dick, B. Gierulski, A., Appl.Phys. B40, 1 (1986)

/46/ Alden, M., Bengtsson, P.-E., Edner, H., Appl. Opt. (1986)

/47/ Zur Loye, A.O., Bracco, F.V., Santavicca, D.A., Proc.Int.Symp. on Diagnostics and Modeling of Combustion in Reciprocating Engines, p. 249, Tokyo (1985)

/48/ Chen, L.D., Roquenmore, W.M., Comb. and Flame (1986)

/49/ Miake-Lye, R.C., Toner, S.J., Comb. and Flame (1986)

/50/ Cool, T., Appl.Opt., 23(10), 1559 (1984)

/51/ Tjossen, P.J.H, Cool, T. A., 20th Symp. (Int.) on Combustion, p. 1321, Pittsburgh (1985)

/52/ Smyth, K. C., Taylor, P. H.,Chem.Phys.Lett., 122, 518-22 (1985)

/53/ Hart, L.P., Smith, B.W., Omenetto, N.,Spectrochim.Acta, 40B, 1637 (1985)

/54/ Smyth, K.C., Mallard, W.G., J. Chem.Phys. 77, 1779 (1982)

/55/ Smith, B.W., Hart, L.P., and Omenetto, N., Anal.Chem., 58, 2147-51 (1986)

/56/ Omenetto, N., Berthoud, T., Cavalli, P., Rossi, G., Appl. Spectrosc., 39, 500 (1985)

/57/ Goldsmith, J.E.M., 20th Symp. (Int.) on Combustion, p. 1331, Pittsburgh (1985)

ANGEWANDTE
CHEMIE
Volume 26 · Number 1
January 1987
Pages 38–58

International Edition in English

Reprint

Laser Chemistry—What is Its Current Status?

By Karl Kleinermanns and Jürgen Wolfrum*

In recent years, various methods have been developed to observe and to influence the course of chemical reactions using laser radiation. By selectively increasing the translational, rotational, and vibrational energies and by controlling the relative orientation of the reaction partners with tunable infrared and UV lasers, direct insight can be gained into the molecular course of the breaking and re-forming of chemical bonds. Examples for the application of lasers include the synthesis of monomers such as vinyl chloride and polymers such as polyethylene, the synthesis of biologically active substances such as vitamin D_3, the separation of isotopes, the removal of impurities, the production of catalysts, glasses, and ceramics, and the deposition and ablation of material on surfaces. Finally, several applications of lasers in medicine are discussed.

1. Introduction

Irradiation with light can strongly affect the course of chemical reactions. The best known example is photosynthesis in plants. In addition, electromagnetic radiation is the most important aid in determining the structure, properties, and chemical behavior of molecules. In spite of great successes, spectroscopy with conventional light sources has not been able to answer many interesting questions. Only the practical realization of the principle of stimulated emission (first formulated by *Einstein*[1]), in the microwave region in 1955[2] and in the visible spectral region in 1960,[3] led to a decisive advance. As in many other areas of science and technology, the laser has also created numerous new possibilities for chemistry.[4] Particularly the introduction of tunable laser light sources, such as the dye laser,[5] and the development of linear and nonlinear optical techniques, such as laser-induced fluorescence (LIF), resonant multiphoton ionization (REMPI), coherent anti-Stokes Raman scattering (CARS), laser Raman spectroscopy on surfaces (SERS), photoacoustic spectroscopy (PAS), laser magnetic resonance spectroscopy (LMR), and Doppler-free absorption spectroscopy, allow virtually every spectroscopic state of an atom or molecule to be observed with high resolution, from the far infrared with wavelengths of several millimeters to the vacuum ultraviolet with wavelengths in the nanometer range.[6] The higher sensitivity allows observation of single atoms in ultramicroanalysis. Further, laser spectroscopy allows nonintrusive observation of rapidly changing chemical processes, such as combustion with high temporal, spectral, and spatial resolution.[7]

The high power of laser light sources within a narrow spectral region allows specific degrees of freedom of molecules to be excited in order to initiate or to influence reactions and to investigate the reaction products state-selectively. In this way, the relative velocity of reaction partners can be adjusted very precisely over a wide region, molecules allowed to rotate faster or slower, and bonds in a molecule stretched to various degrees; with polarized laser light, the mutual orientation of chemical species during the course of a reaction can be specified. Moreover, short-lived "transition states" of chemical reactions can be observed. In the first part of this article, the selective excitation and observation of chemical transformations with the aid of laser radiation is exemplified by reactions in the gas phase.

The progress achieved in laboratory investigations in controlling the course of reactions by excitation with laser light suggests that the newly developed methods could also be used for the production of new products or the improvement of syntheses. However, it was found that, for large-scale reactions performed in chemical reactors, the energy exchange between molecules and the deactivation of excited molecules take place very quickly and that "memory" effects with respect to the initially prepared state only rarely influence the reaction. In spite of these limitations, a number of interesting laser-induced chemical processes have been described in recent years. In the second part of this article, selected examples of the application of high-power lasers for initiating chemical transformations are presented.

2. Influence of the Specific Excitation of Molecular Degrees of Freedom on the Course of Chemical Reactions

The dependence of the rate of chemical reactions on the energy supplied is daily laboratory experience for the chemist. Often, the energy of the reaction partners can be represented by a temperature and the dependence of the reaction rate on temperature by a simple Arrhenius equation. The Arrhenius parameters obtained in this way do not, however, provide any information on the contribution of specific degrees of freedom of the reaction partners to overcoming the energy barrier of the reaction. In the following examples, reactions in the gas phase are used to show how information on the molecular course of reaction can be obtained in experiments with lasers.

[*] Prof. Dr. J. Wolfrum, Dr. K. Kleinermanns
Physikalisch-Chemisches Institut der Universität
Im Neuenheimer Feld 253, D-6900 Heidelberg (FRG)

  0570-0833/87/0101-0038 $ 02.50/0

2.1. Translational Excitation

Chemical reactions of fast ("hot") atoms from nuclear recoil and photolysis processes have long been investigated by analysis of their stable end products.[8] On bombarding ^{6}Li with neutrons, for example, tritium (^{3}H) atoms with a recoil energy of 2.7 MeV are formed. Collisions then retard these fast ^{3}H atoms to the "chemical" energy range around 20 eV to give a broad, continuous distribution of velocities. Thus the reaction energy cannot be controlled directly. Narrow-bandwidth laser light of high intensity and short pulse length (10^{-8} s), on the other hand, allows high concentrations of atoms with defined velocities to be produced by photodissociation (Fig. 1).

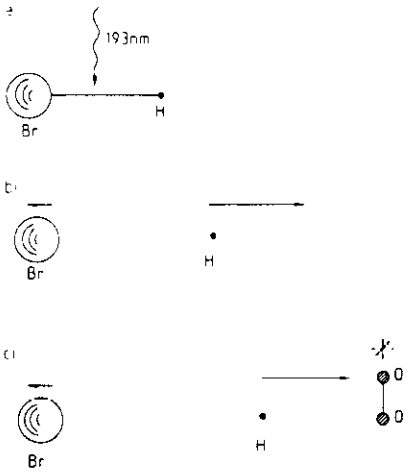

Fig. 1. Production of fast hydrogen atoms by photolysis with short-wavelength laser radiation. a) The ArF excimer laser photolyzes a suitable hydrogen-atom precursor such as HBr. b) The photolysis energy $h\nu$ is considerably greater than the dissociation energy of HBr and is more than 98% converted into the translational energy of the hydrogen atom, because the heavy bromine atom is more or less stationary compared with the light hydrogen atom. The hydrogen atom then passes with a velocity of 23 km s^{-1} through the reactor until it collides with an oxygen molecule. The average velocity of the oxygen molecule at room temperature is more than two orders of magnitude smaller than that of the hydrogen atom, so that, to a good approximation, the velocity of H relative to O_2 is the same as the velocity of the hydrogen atom. In this way, a collision energy of 251 kJ mol^{-1} is obtained. By changing the photolysis wavelength and the hydrogen-atom precursor, the velocity of the hydrogen atom can be set over a wide range and collision energies from 80 kJ mol^{-1} to over 400 kJ mol^{-1} can be attained.

As an example, the reaction (a) of translationally excited hydrogen atoms H^T with oxygen is examined. This endothermic reaction leads to the formation of two reactive radicals and is the most important chain-branching step in numerous oxidation and combustion processes.[9, 14]

$$H^T(^2S) + O_2(^3\Sigma_g^-) \longrightarrow OH(^2\pi, v, J, f) + O(^3P) \qquad (a)$$

$\Delta H_0 = 69.9$ kJ/mol

v = vibrational quantum number,
J = rotational quantum number,
f = fine structure quantum number

One experimental setup that can be used to investigate reaction (a) and other reactions of fast atoms with molecules is shown in Figure 2. It consists of a flow system

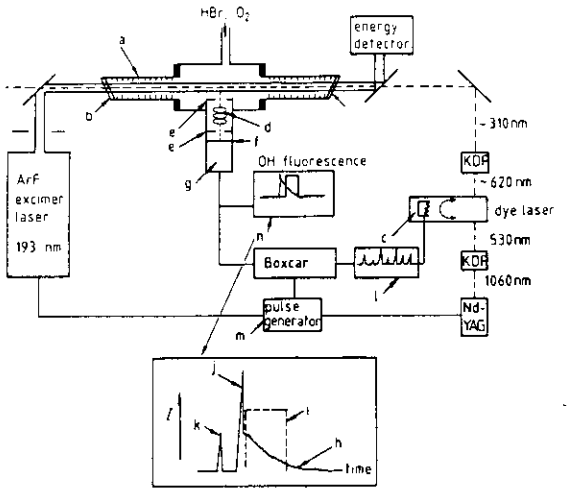

Fig. 2. Setup for state-specific and time-resolved investigation of reactions of fast atoms with molecules. The photolysis pulse of the ArF excimer laser (193 nm, 200-mJ pulse energy, 15-ns pulse length) and the analysis pulse of the Nd-YAG laser-pumped dye laser pass through the flow reactor coaxially. The reactor is equipped with collimators (a) in the side-arms, which partially remove the laser light scattered at the quartz windows (b). The analysis laser (0.2-cm^{-1} spectral band width, 12-ns pulse length and 0.1–1-mJ pulse energy) employs the laser dye Rhodamine 640. After frequency doubling (potassium diphosphate crystal), the OH radicals can be excited between 306 and 311 nm (tuning by a "grating" (c)). If the wavelength of the analysis laser is changed, the OH radicals absorb and fluoresce at different excitation wavelengths with varying strength, depending on how favorably the corresponding vibrational-rotational fine-structure state is populated by reaction (a). The fluorescence intensity is detected by a photon detector (g) after passing a lens system (d), collimators (e), and a filter (f). This intensity is a measure of the probability with which a particular OH state is excited by the chemical reaction. The signal current (h) released by the fluorescence at the photomultiplier is summed over many laser pulses using a "boxcar" system in an adjustable time region ("box") (i) beyond the interferring stray light (j, k) and then plotted against the analysis laser wavelength on a recorder (l). The analysis time is varied by starting the two lasers with two trigger pulses, time-delayed with respect to each other. Typical analysis times are 40–100 ns at a partial pressure of 5 mbar HBr and 50 mbar O_2. Owing to the short analysis times and the low concentrations of species, one avoids secondary reactions and deactivation of the fast hydrogen atoms and the excited OH radicals by collisions.

combined with a photolysis laser for producing hot hydrogen atoms and a frequency-doubled dye laser for state-specific, time-resolved detection of the OH radical by means of laser-induced fluorescence (LIF). The measurements show that the OH radicals formed in reaction (a) are rotationally very highly excited[10] (Fig. 3).

In order to compare the experimental rotational distribution with a calculated rotational distribution, the motion of the three atoms over a quantum-mechanically (ab initio) calculated H–O_2 potential hypersurface[11] is followed by stepwise integration of the classical equations of motion for various initial conditions (relative velocities, orientation of the collision partners, rotational and vibrational states of O_2).[12] The greater part of the relative translational energy of the reactants is converted into rotational energy of the product OH, in qualitative agreement with experimental results. However, careful quantitative comparison still shows distinct discrepancies (Fig. 3). For a collision energy of 251 kJ/mol (ca. 60 kcal/mol), the theoretical cross section, i.e., the reaction probability integrated over the collision parameters and other initial conditions, is a factor of 3 smaller than the experimental value. This discrepancy is particularly disturbing because the absolute

rate constant of reaction (a) at high temperatures, a sensitive parameter, for example in the mathematical modeling of combustion processes,[9] needs to be known exactly. The larger cross section found experimentally has been confirmed by more recent measurements[13] of the thermal rate constants $k_1(T)$ at higher temperatures (1500–2500 K); thus, the values calculated using the quantum-mechanical potential hypersurface are much too low.

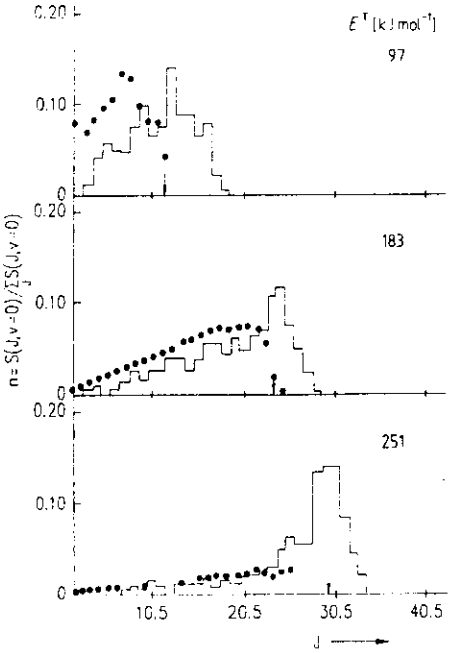

Fig. 3. Rotational excitation of OH (v=0) produced by reaction (a). The points show the experimental, the curve (histogram) the calculated distribution at collision energies of 97, 183, and 251 kJ mol^{-1}. At very high excitation (J > 23.5), OH (v=0) predissociates from the $^2\Sigma$ state and no longer fluoresces. The arrows show the maximum rotational excitation obtainable for complete conversion of the reaction energy into rotational energy. The collision energies E^T given here have an uncertainty of ±10%.

The fine structure distribution also provides interesting information on reaction dynamics. For instance, the OH λ-doublet excitation shows that the π^+ components are favored.[10, 15] As explained in Figure 4, this means that, at high collision energies, the H^T–O_2 reaction proceeds mainly on the initial plane. By using polarized photolysis and analysis laser light, the flight direction of the photolytically produced hydrogen atoms can be specified and the orientation of the OH product radicals relative to the flight direction of the hydrogen atoms measured. Strong polarization effects were found experimentally[16]—the OH angular momentum vector, J_{OH}, lies perpendicular to the velocity vector of the hydrogen atoms, v_H (Fig. 5).

2.2. Rotational Excitation

Because rotational states are energetically very close together and can be rapidly deactivated, the influence of reactant rotation on the course of reactions is investigated using an arrangement with crossed molecular beams to avoid interfering collision processes. Infrared transitions of an HCl or HF molecular laser are used for selective excitation of rotational states in HCl and HF molecules. Typ-

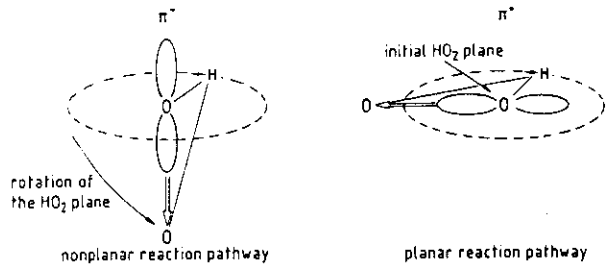

Fig. 4. The physical difference between the two λ-doublet components π^+ and π^- arises from interaction of the electronic spin-orbit momentum with the rotation of the molecule. For fast rotation of the OH radical, the unpaired electron in the p orbital on oxygen is no longer able to follow the movement of the atomic nuclei. If the p orbital lies in the OH rotational plane, the electron distribution on the oxygen atom changes, becoming increasingly spherical. In contrast, for a π^- configuration, the oxygen atom moves in the nodal plane of the p orbital and thus continues to "see" a dumbbell-shaped electron environment, even for fast rotation. This leads to a splitting of the energies of the π^+ and π^- configurations, which increases with increasing rotational energy. Experimentally, at 183 kJ mol^{-1} collision energy, three OH radicals were found in the π^+ state for each OH radical in the π^- state [15]. This shows that the unpaired electron formed after bond cleavage of O_2 stays in an orbital in the rotational plane of the OH radical. During the reaction, most of the HO_2 complexes do not rotate out of the initial plane, because of the short reaction time at high collision energies.

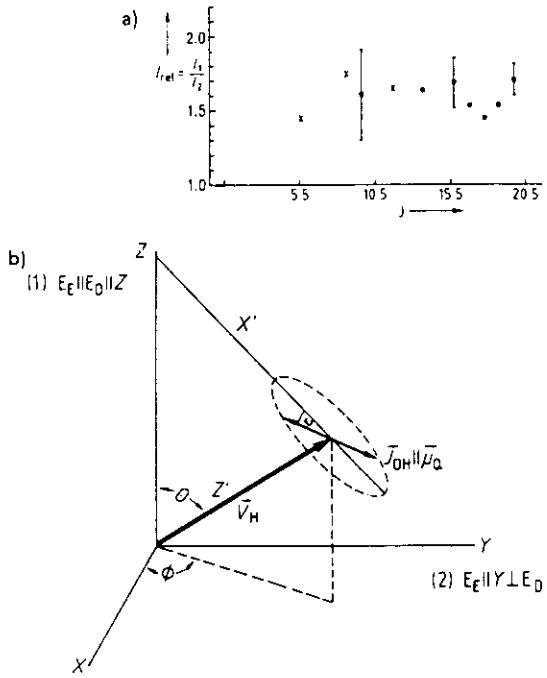

Fig. 5. a) Experimental polarization effects at 251-kJ mol^{-1} collision energy. J is the rotational quantum number; the ordinate is the polarization ratio, I_{rel}, the ratio of the fluorescence signal intensity for polarization of the photolysis laser E_D parallel to the analysis laser E_E and perpendicular to it. The electric vectors of the laser radiation at 193 (×) and 307 nm (•) are rotated independently. b) The laser beams lie parallel to the laboratory X axis, the detector parallel to the Y axis. The molecular coordinates are X′ and Z′; $\vec{v}_H$ is the velocity vector of the hydrogen atoms, and J_{OH} the angular momentum vector in the molecular coordinate system. On excitation of a Q transition (ΔJ = 0) of the OH radical, fluorescence intensities and polarization ratio can be calculated from the projection of the Q transition moments μ_Q ($\| J_{OH}$ for high rotational states) on the laboratory axis [16]. For the orientation $J_{OH} \perp v_H$, the calculation is in agreement with the experimental polarization ratio of 1.60.

ical results are shown in Figure 6. Initially, a decrease in the reaction probability with increasing degree of rotational excitation is observed. A possible explanation is that a particular orientation of the reaction partners, e.g., colinear, often gives the reaction path of lowest energy. With increasing rotation of the molecule, however, the potential forces are less and less able to orient the reaction partners satisfactorily with respect to one another and the reacting atom is increasingly "protected" from the reaction partner. If the rotational excitation is further increased, the steric hindrance plays a lesser role as a result of the rapidly increasing total energy, i.e., the "cone of acceptance" rapidly expands. In addition, because of the higher total energy, more states become accessible on the product side, which leads to a further increase in the reaction probability.

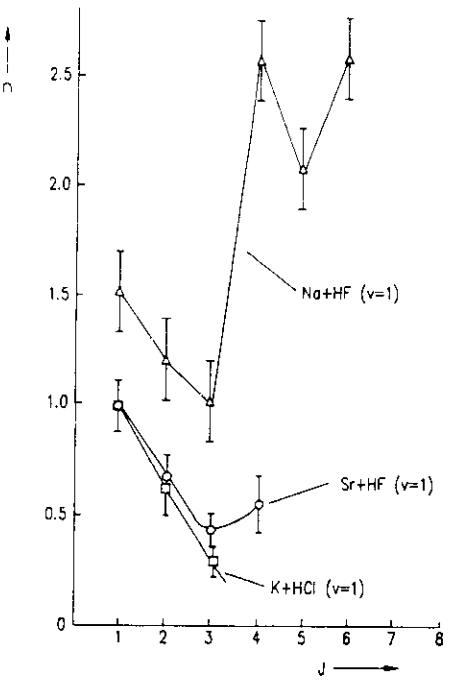

Fig. 6. Investigation of the dependence of the reaction cross section on rotational excitation in the following reactions: K + HCl (v = 1, J) ⟶ KCl + H, Sr + HF (v = 1, J) ⟶ SrF + H, and Na + HF (v = 1, J) ⟶ NaF + H. n = relative reaction cross section; J = rotational quantum number.

If a long-lived intermediate complex is formed during the reaction, the additional rotational energy is distributed statistically over the various degrees of freedom of the product; i.e., "memory" of the energy form of the original excitation is largely lost. Thus, in the reaction

$$Ca(^1S) + HF(X\,^1\Sigma^+, v = 1, J = 0\text{-}7) \longrightarrow CaF(X\,^2\Pi, v', J') + H(^2S)$$

X = electronic ground state

Zare et al.[18] observed statistical vibrational excitation of CaF following selective rotational-vibrational excitation of HF.

With the laser-induced fluorescence technique described in Section 2.1, the rotational states of the products could be investigated for a large number of reactions. For instance, the reactions of $O(^3P)$ atoms with saturated and unsaturated hydrocarbons, amines, and aldehydes lead to OH product radicals with low rotational excitation, which can be attributed to the weak rotary torque involved in the almost colinear, direct abstraction of the hydrogen atom.[19] In contrast, the rotational excitation of OH produced by reaction of excited oxygen atoms $O(^1D)$ with H_2 and HCl is extremely high. With saturated hydrocarbons, one observes overlapping of two distributions. This can be traced to a direct, colinear abstraction path (low rotational excitation) and a parallel reaction path with insertion of $O(^1D)$ into the C-H bond (high rotational excitation via decay of a highly excited "alcohol").[20]

2.3. Vibrational Excitation

A connection between chemical reactivity and the efficiency of the vibrational energy exchange between molecules was first postulated by *Franck* and *Eucken* more than 50 years ago.[21] However, systematic investigations in this area only became possible through the development of powerful and tunable infrared lasers.[22, 23] The reaction of hydrogen molecules with hydrogen atoms or their isotopes, as the simplest example of a bimolecular reaction of neutral species, is particularly suitable for a theoretical investigation of the influence of selective vibrational excitation of reacting species (see energy diagram, Fig. 7). The energy required for vibrational excitation of the hydrogen molecule considerably exceeds the Arrhenius activation energy (E_a), the threshold energy (E_0), and the height of the energy barrier (E_c) of the reaction in the vibrational ground state.

E_c was first calculated quantum mechanically by *London*[24] more than half a century ago. The value he obtained is not very different from the results of modern ab initio calculations.[25] This good agreement disappears, however, when a more exact calculation is performed according to *London*'s valence bond method.[26] The classical methods for the study of reaction kinetics are difficult to apply to this reaction, because known concentrations of vibrationally excited hydrogen molecules have to be produced and detected. Only the application of CARS spectroscopy has allowed direct, quantitative detection of hydrogen molecules in selected vibrational and rotational states. It was shown that when the H_2 molecule is excited to the first vibrational state, only about a third of the vibrational energy is used to overcome the energy barrier E_c.[27] Thus, the reaction of vibrationally excited hydrogen molecules still shows an energy barrier, whose height can be predicted both from classical and from quantum-mechanical calculations of the course of reaction on the ab initio potential hypersurface, in good agreement with the experiments.[28] More recent measurements of the absolute value of the rate constant by CARS spectroscopy[29] agree well with the results of quasi-classical trajectory calculations.[30] This is also the case for the results of experiments with translationally excited hydrogen atoms.[31]

The results obtained from study of the hydrogen exchange reaction on the efficiency of a selective vibrational excitation cannot be simply transferred to similar reac-

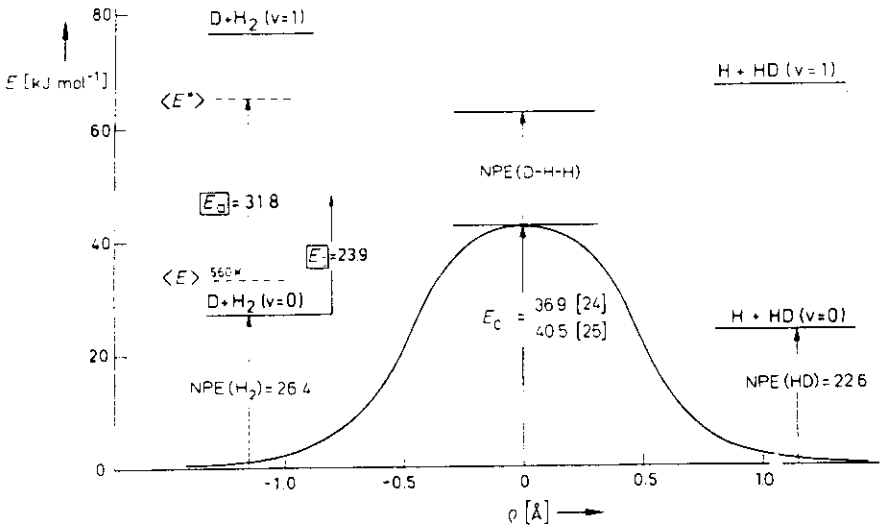

Fig. 7. Characteristic energy requirements of the hydrogen exchange reaction. E_a is the Arrhenius activation energy, E_0 the minimum collision energy that leads to reaction (threshold energy), and E_c the height of the potential energy barrier of the reaction in the vibrational ground state. $\langle E \rangle$ is the average thermal energy of all binary collisions per unit time and $\langle E^* \rangle$ the average kinetic energy of all collisions per unit time that lead to reaction. NPE is the zero point energy of vibration, ρ the reaction coordinate.

tions. Thus, investigations of the also thermoneutral reaction

$$^{37}Cl + H^{35}Cl\ (v = 1) \longrightarrow H^{37}Cl\ (v = 1,0) + {}^{35}Cl$$

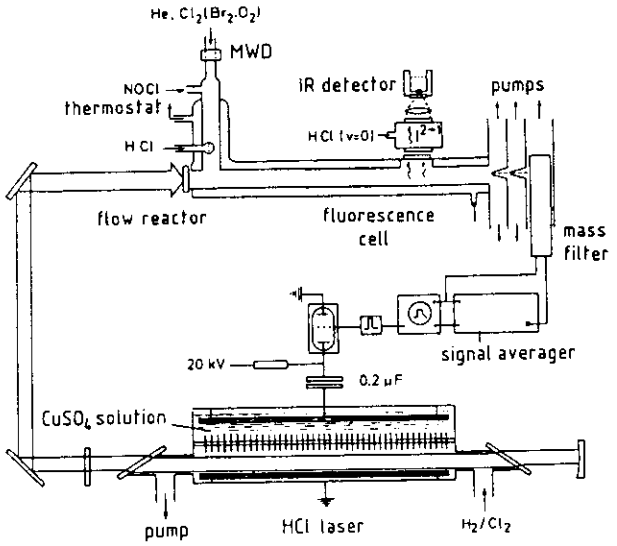

Fig. 8. Experimental setup for the investigation of reactions of vibrationally excited hydrogen halide molecules with the aid of time-resolved molecular-beam mass spectrometry. A discharge flow reactor is coupled through a molecular beam sampling system directly to the ion source of a quadrupole mass spectrometer. The HCl molecules are vibrationally excited isotope selectively by the infrared radiation of an HCl laser. The degree of the vibrational excitation is determined from the intensity of the infrared emission. A filter cell with cold HCl absorbs the infrared radiation of the transition HCl (v = 1) → HCl (v = 0) resonantly and transmits the wavelengths of the transition HCl (v = 2) → HCl (v = 1). From the ratio of the infrared intensity with and without the HCl cell, the degree of excitation of the HCl molecules can be determined directly. Chlorine, bromine, or oxygen atoms, which are produced by dissociation in a microwave discharge (MWD), react in the flow system with the vibrationally excited HCl molecules. The reaction products are detected mass spectrometrically.

demonstrate very effective use of the vibrational energy for overcoming the energy barrier.[32] The experimental setup for investigation of the reaction is shown schematically in Figure 8. The experimental rate constants of the reaction in the states HCl (v = 0) and HCl (v = 1) are given in Figure 9. The high efficiency with which the vibrational energy is used to overcome the energy barrier causes the chemical reaction, with increasing temperature, to proceed preferentially via the excited vibrational states. Thus, the temperature dependence of the reaction deviates significantly from that predicted by an Arrhenius equation. The dynamics of the reaction have been simulated by classical, semiclassical, and quantum-mechanical calculations.[33] Particularly

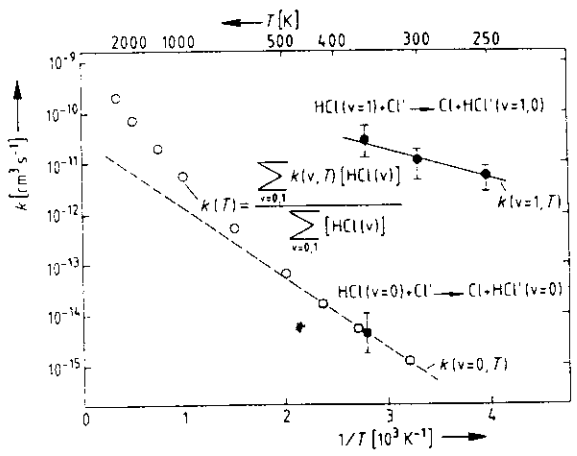

Fig. 9. Contributions of the vibrational ground state (v = 0) and the first excited state of HCl (v = 1) to the rate constant of the reaction Cl + HCl(v) → Cl + HCl(v'). The strong rise in reaction rate after vibrational excitation has the effect that, at higher temperatures ($T > 500$ K), marked deviations from the Arrhenius line are observed. Measured rate constants: □, ■ for HCl (v = 0), ● for HCl (v = 1); ○, calculated rate constants from the contributions of HCl (v = 0) and HCl (v = 1).

in very strongly endothermic reactions can vibrational excitation be used effectively for increasing the rate of reaction. Thus, in the reaction[34]

$$Br + HCl(v) \longrightarrow HBr(v=0) + Cl$$

an increase in the reaction rate constant by more than ten orders of magnitude can be obtained by vibrationally exciting the HCl molecule from $v=0$ to $v=2$. This dramatic increase in the rate constant can be used to separate chlorine isotopes (Fig. 10). ^{35}Cl atoms from HCl can be transformed in this way into $Br^{35}Cl$, which because of its different chemical and physical properties can be readily separated from the reaction mixture.

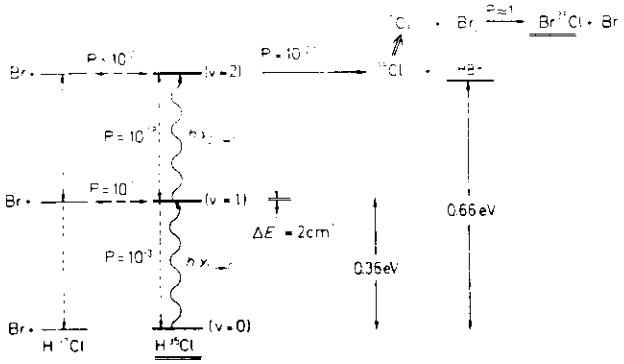

Fig. 10. Energy diagram for the reaction of Br atoms with isotope-selectively excited HCl molecules. P gives the probability for the transfer of vibrational energy between laser-excited $H^{35}Cl$ and $H^{37}Cl$ and for the course of a reaction in the various collision processes, respectively. The Br atoms react preferentially with $H^{35}Cl$ ($v=2$). The resulting ^{35}Cl atoms further react with molecular bromine to give easily separated $Br^{35}Cl$. $\Delta E'$ is the energy difference between $H^{35}Cl$ ($v=1$) and $H^{37}Cl$ ($v=1$).

Investigations of the reactions of polyatomic molecules in specifically excited vibrational states are much more difficult to perform. One main problem is the decoupling of the vibrational energy-transfer processes from the processes leading to reaction. Interesting model molecules are substituted methanes.[35] For example, Figure 11 shows the energy flow in CH_3F after excitation of the CF stretching vibration ν_3 with a CO_2 laser. By almost resonant vibrational energy transfer, subsequent collisions rapidly populate higher states ($2\nu_3$, $3\nu_3$) of this stretching vibration, resulting in a "metastable," mode-selective excitation of the CF stretching vibration. Through local Coriolis resonance between the third overtone of ν_3 and the CH stretching vibration ν_4, part of the energy can be channeled into this CH stretching vibration. Simultaneously, depending on pressure, CH bending vibrations (ν_6, ν_2, ν_5) are excited by collisions with further molecules, the excitation energy being provided by the thermal energy of the surrounding gas. In the subsequent resonant vibrational energy transfer, higher states of these vibrations can be populated, from which the CH stretching vibration ν_1 is reached by Fermi resonance. Examples of reactions of vibrationally excited polyatomic molecules are the reaction of laser-excited ozone molecules with nitric oxide[23,36] and that of fluorine with unsaturated hydrocarbons in a low-temperature matrix.[37]

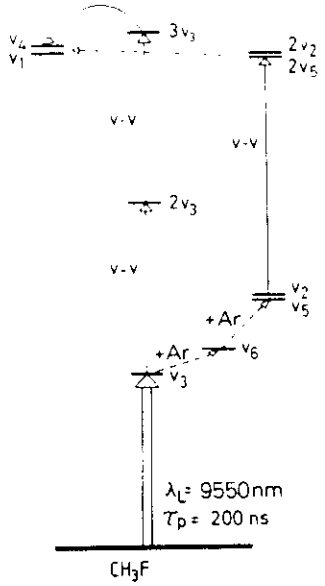

Fig. 11. Paths for the collision-induced intramolecular vibrational energy transfer in CH_3F. Laser radiation with wavelength λ_L and pulse length τ_p.

2.4. Electronic Excitation

In the following, no attempt is made to give a detailed overview of the reaction behavior of electronically excited atoms and molecules. Rather, using selected examples, it is shown how reactants can be selectively oriented with respect to one another, regions of "transition states" probed, and reaction rate constants for high excitation far above the reaction threshold investigated using electronic excitation with laser light.

At some stage in the course of a chemical reaction, new bonds are formed and old bonds broken, so that neither "reactants" nor "products" are in effect present. The direct investigation of such "transition states" has long been the chemist's dream. Figure 12a shows that a range of such transition states can be excited with laser light having a wavelength that is nonresonant with the reactant or product states. Among the reactions investigated[38] was that of $K(4s^2S)$ atoms with NaCl using excitation with laser light in a crossed molecular beam experiment (Fig. 12b).[39] As the reaction partners approach, the states of the species mutually "perturb" each other and their energy changes. When the wavelength of the laser light is finally resonant with the $Na^*(3p^2P)$-KCl state, excitation to this state occurs and light emission at $\lambda = 589$ nm ($Na^*(3p^2P) \rightarrow Na(3s^2S)$ transition, sodium D-line) is observed, as shown in Figure 13 as a function of excitation wavelength. Emission at 589 nm occurs even on excitation with longer-wavelength light. The missing energy comes from the exothermicity of the reaction and thermal energy of the reactants. By improving the signal-to-noise ratio of the measurements, it should be possible to recognize structures in the spectrum and identify areas of longer residence time of the complex on the ground-state hypersurface from the intensity maxima.

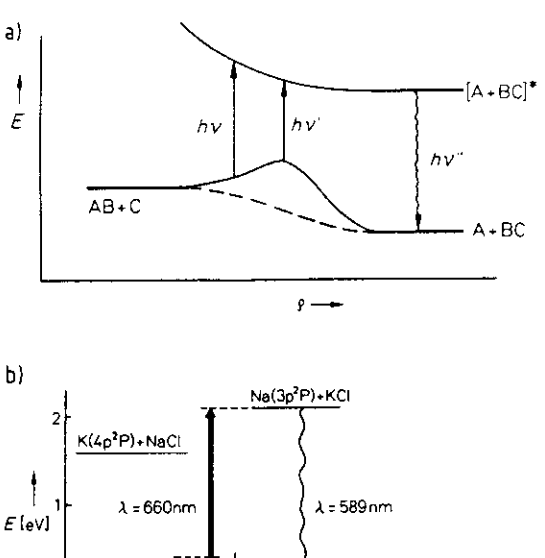

Fig. 12. a) "Transition state" spectroscopy of an exothermic reaction. The emitted frequency ν'' is higher than the radiated frequencies ν or ν'. The missing energy comes from the heat of reaction and the thermal energy of the reactants. b) Energy level diagram of the K-NaCl reaction. 1750 cm^{-1} corresponds to the heat of reaction.

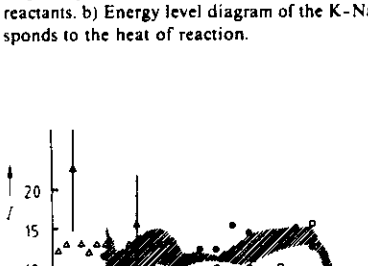

Fig. 13. Luminescence signal from the reaction K $(4s^2S)$ + NaCl → $Na^*(3p^2P)$ + KCl, occurring in crossed molecular beams, as a function of the excitation wavelength. Only when all three beams are present *simultaneously* (K, NaCl, and laser beam) is intense luminescence at 589 nm observed. The dotted area in the diagram gives the average of two or more measurements. The differently marked data points refer to measurements on different days.

In addition to emission from laser-excited "transition states," emission from *chemically* excited intermediate complexes also has been observed. As Figure 14 shows, *Polanyi* and co-workers[40] were still able to detect fluorescence from the reaction

$$F + Na_2 \longrightarrow FNaNa^{**} \longrightarrow NaF + Na^*(3p^2P)$$

far from the sodium D-line. This "wing" fluorescence originates from Na* near NaF (and hence also from $FNaNa^{**}$). The higher intensity of the long-wavelength "wing" is due to the fact that the upper and lower potential surfaces tend to lie closer together at intermediate configurations (cf. Fig. 12a).

Following excitation into "repulsive states," structured emission spectra were observed, even though a rapid dissociation follows the excitation.[41,42] These fluorescence

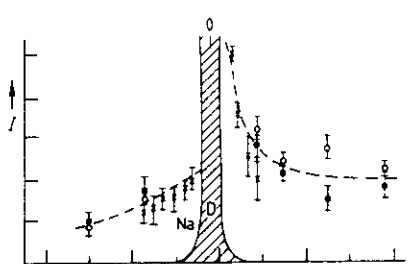

Fig. 14. Emission of the "intermediate complex" $FNaNa^{**}$ formed in the reaction F + Na_2 → NaF + Na*.

spectra provide information on the previously inaccessible temporal course of a bond rupture. From the frequency shift of the emission lines relative to the excitation wavelength, the vibrational frequency in the electronic ground state is obtained up to the vicinity of the dissociation limit (Fig. 15). Fluorescence occurs when the continuum wave function of the upper (repulsive) potential surface overlaps favorably with vibrational wave functions of the lower (bonding) electronic ground state. In a direct dissociation, later times in the course of photodissociation correspond to more elongated bonds and hence emission to higher vibrational states of the electronic ground state (cf. Fig. 15, vertical optical transition). For example, following excitation at $\lambda = 266$ nm, CH_3I dissociates within femtoseconds to CH_3 and I. Although the dissociation is about six orders of magnitude faster than the spontaneous emission, fluorescence is still observed. Optical transitions to highly excited states of the CH_3 "umbrella vibration" of CH_3I are only observed in combination with excited CI stretching vibrations.[42] This behavior can be attributed to the fact that the C-I bond has to be elongated considerably before the methyl group opens from the tetrahedral geometry in CH_3I to the planar form in the CH_3 product radical.

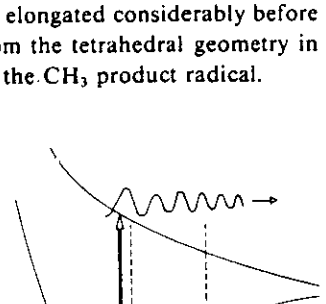

Fig. 15. Scheme for laser-induced fluorescence spectroscopy on repulsive surfaces. A molecule is excited by a UV laser into a dissociative state. In spite of rapid decay, fluorescence (dotted line) occurs when continuum wave functions and vibrational wave functions favorably overlap.

The influence of the orientation of the reaction partners with respect to one another, observed indirectly in experiments involving rotational excitation of the reactants, can also be observed directly using laser techniques. With polarized laser light, molecules having a particular orientation can be selectively excited, since the probability for ab-

sorption of light is at a maximum when the transition dipole moment is parallel to the electric field vector. With this method, *Zare* and co-workers[17h,43] were able to show that the reaction of polarized, excited iodine molecules with indium atoms occurs faster in "head-on" collisions than in a "side-on" attack (Fig. 16).

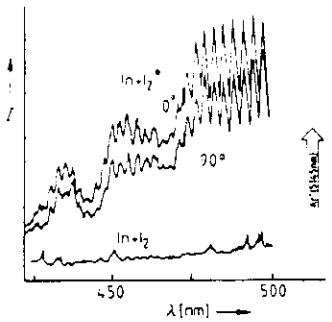

Fig. 16. LIF spectrum of InI from the reaction In + I_2^* → InI + I. Iodine was excited into the B($^3\Pi$) state with a linearly polarized Ar^+ ion laser at 514.5 nm. The transition moment here lies parallel to the iodine molecular axis. On orienting the electrical vector parallel to the In beam (0°), the reaction proceeds more rapidly ("head-on" collisions) than for perpendicular orientation (90°). The lowest curve gives the fluorescence measured upon switching off the laser.

Different wavelengths of light can be employed to selectively excite molecules having different orientations. Thus, SrF from the reaction of strontium atoms with vibrationally excited HF (excitation to v = 1, J = 1 by a polarized HF infrared laser) is more highly vibrationally excited after a side-on than after a head-on collision. Calculations show[44] that when the reaction occurs at the energetically more favorably angled alkali-metal-HF orientation, energy is preferentially transferred to the internal degrees of freedom of the product molecule.

Polarized laser light can also be used to influence the orientation of the electron orbitals in atoms. The excitation of Ca($^1S_0$) to Ca($^1P_1$) results in transfer of charge from a spherical s orbital to a dumbbell-shaped p orbital. The transition moment lies in the direction of the Ca p orbital, so that this orbital is aligned with the electrical vector of the laser light. In the reaction of Ca($^1P_1$) with HCl, the CaCl A($^2\Pi$) state is formed preferentially when the calcium p orbital is aligned perpendicular to the calcium beam. In contrast, the CaCl B($^2\Sigma^+$) state is excited preferentially when the Ca p orbital lies parallel to the calcium beam (formation of a σ_p orbital in CaCl).[45] "Memory effects" on the initial state have also been observed in the reaction of O(^{3}P) atoms with saturated hydrocarbons. *Luntz* and *Andresen*[19a] showed that O($^3P_2$) atoms give rise preferably to the $^2\Pi_{3/2}$ spin-orbit states of the OH radical for symmetry reasons.

By electronic excitation of molecules with lasers, specific rate constants, $k(E)$, for unimolecular reactions can be measured directly. *Troe* and co-workers have investigated the isomerization of various cycloheptatrienes in their electronic ground states by means of thermal isomerization[46] as well as stationary[47] and direct, time-resolved[48] photoisomerization. On excitation of cycloheptatriene molecules in the ultraviolet spectral region, light absorption ($S_0 + h\nu \rightarrow S_1$) is followed by rapid internal conversion to vibrationally highly excited levels of the electronic ground state (S_0^*, Fig. 17). The hot cycloheptatriene molecules isomerize faster with decreasing wavelength. From the increase in the absorption signal with time, the specific rate constants could be determined directly. Figure 18 shows that a statistical model of $k(E)$ is in good agreement with the experimental results.

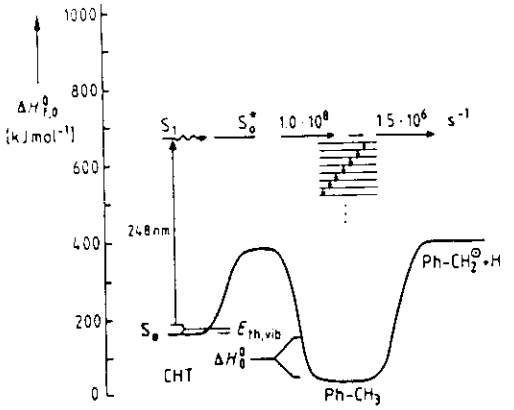

Fig. 17. Potential energy scheme for the photoisomerization of cycloheptatrienes. Electronic excitation into the S_1 state is followed by rapid internal conversion to vibrationally excited CHT in the electronic ground state (S_0), which with rising excitation energy isomerizes increasingly faster to toluene.

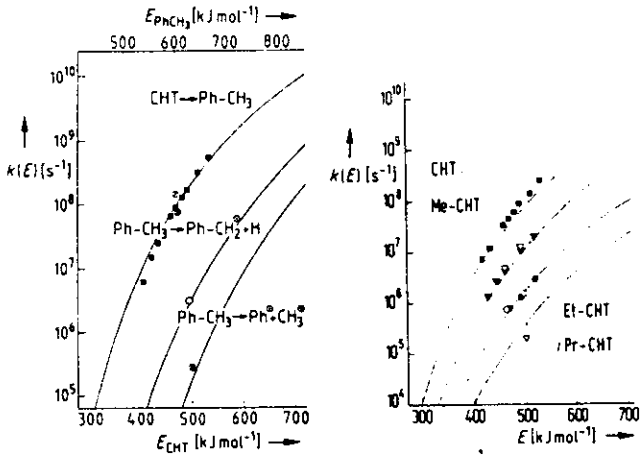

Fig. 18. Specific rate constants, $k(E)$, for the unimolecular isomerization of cycloheptatriene. ○, ⊘, ⊗, ▽, ■, direct, time-resolved measurements by excitation with laser light; ●, ▼, ■, stationary photoisomerization experiments (Stern-Volmer extrapolation); solid line, statistical calculation according to RRKM theory.

3. Lasers in Synthesis

It would seem obvious to use the methods described for the selective control of chemical reactions for making new products or improving synthetic procedures. Under the typical conditions of industrial chemical processes (high pressures, reactions in the liquid phase, large molecules), however, a selected molecular state cannot, in most cases,

be held stable until the actual reaction stage. The exchange of energy between the degrees of freedom within a molecule and between various molecules usually occurs on a time scale of 10^{-13} to 10^{-10} s, whereas the reaction times themselves are considerably longer. On the other hand, nonthermal isomer and isotope distributions as well as nonthermal radical concentrations from laser-induced dissociation and isomerization processes can readily be maintained under industrial chemical conditions and used for producing new or appreciably purer products or for producing products with lower energy consumption. Here, the use of the laser offers a number of advantages over conventional light sources: (1) extension of the available range of wavelengths; (2) the selective excitation of just one kind of molecule (e.g., for isotope separation or ultrapurification), because of the narrow spectral bandwidth of the laser light; (3) spatially and temporally controllable, homogeneous excitation of the reaction volume, because of the possibilities of pulsed operation and strong collimation; (4) the possibility of multiphoton excitation, because of the high power density.

As shown in Figure 19, Hg or Xe lamps are preferable as light sources for industrial photochemistry both in terms of investment and operational cost as well as in terms of maintenance expenditure, long-term power, and lifetime. For economic application of lasers in this area, the effective cost of the photons must lie considerably below that of the desired product (Fig. 20). One should remember that, generally, the product price is determined only to a small extent by the photochemical step involved in the production process and that techniques employing lasers have to compete not only with conventional photochemical processes, but also with other routes of synthesis. Optimally, the use of lasers should result in several improvements simultaneously, such as cheaper starting materials, fewer or more valuable side products, and fewer or cheaper process steps. In particular, the production of cheap mass-produced chemicals by the use of lasers is only worthwhile if very high quantum yields (number of product molecules produced per photon generated) can be achieved in radical chain reactions.

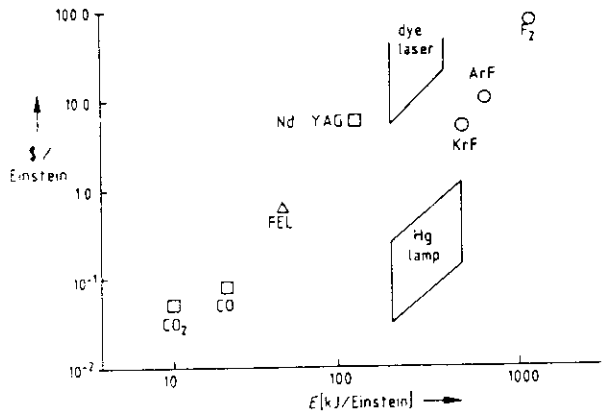

Fig. 19. Photon costs for laser light as a function of photon energy. 1 Einstein is 1 mole of light quanta. FEL = free electron laser. Conventional lamps are at present considerably more inexpensive as light sources than lasers.

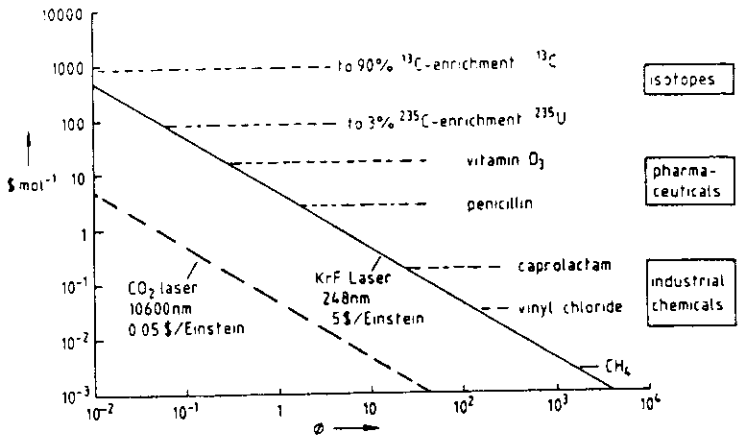

Fig. 20. Influence of quantum yield on product cost. The ordinate gives the cost in dollars per mole of product for conventional chemical syntheses. The application of lasers for production of cheap mass-produced chemicals is only economical at very high quantum yields, Φ.

3.1. Laser-Induced Radical Chain Reactions

Vinyl chloride (VC), the monomer of PVC, is produced industrially mainly by thermal cleavage of HCl from 1,2-dichloroethane (DCE) in a chain reaction. With a worldwide production of over 25×10^6 metric tons per year, VC is one of the leading products of chemical industry in terms of quantity. The advantage of photolytic over thermal initiation of the chain reaction is that the unimolecular process

$$C_2H_3Cl_2 \xrightarrow{+\text{inert gas}} C_2H_3Cl^{\odot} + Cl^{\odot}$$

is rate-determining with a low energy barrier. This leads to a low activation energy for the overall reaction and hence to lower reactor temperatures, higher conversions, and fewer side products. The use of laser radiation to initiate the chain reaction also permits detailed investigations of the reaction kinetics. Radicals may thereby be produced in

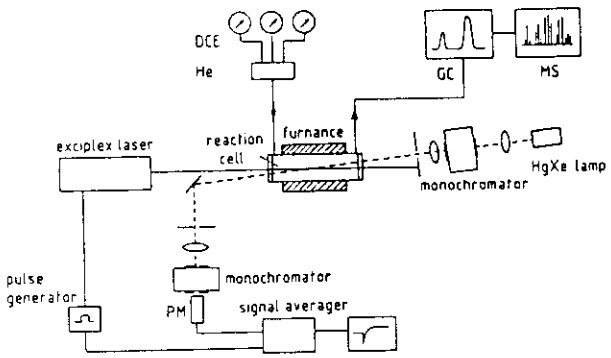

Fig. 21. Experimental setup for the investigation of laser-induced radical chain reactions for the synthesis of VC. The products are detected by time-resolved UV spectroscopy, gas chromatography (GC), and mass spectrometry (MS). PM = photomultiplier.

a wide concentration range and the reactions followed as a function of time. Figure 21 shows the experimental setup required. The formation of vinyl chloride can be followed

directly by time-resolved UV spectroscopy. The entire spectrum of products is recorded with the aid of a GC-MS system. The experimental data can be compared with those obtained from a kinetic model, which for a given temperature and pressure, simulates the whole course of the reaction (Fig. 22) by using a system of coupled differential equations for the elementary chemical steps. From a comparison of the experimental data with the predictions of

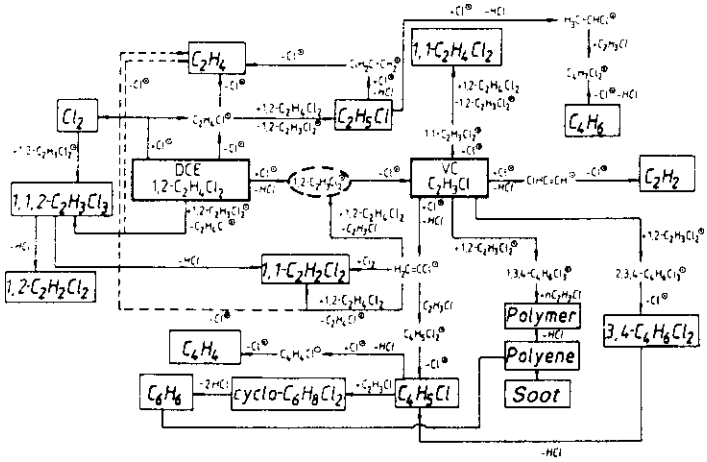

Fig. 22. Reaction paths for the cleavage of hydrogen chloride from dichloroethane, $1,2\text{-}C_2H_4Cl_2$, in a laser-induced chain reaction.

the model, missing rate constants of selected elementary steps can be determined. The pressure and temperature dependence of the laser-induced VC formation can then be used to predict the efficiency of conversion of DCE to VC for industrial conditions. The calculations show that laser photocatalysis results in a clear increase in the efficiency. The addition of chain carriers such as chlorine can increase the quantum yields by over 10^5. A pilot plant for the laser-induced conversion of DCE to VC, which is presently under construction, is shown schematically in Figure 23. DCE is first heated in a tubular reactor. A segment of the reactor is then irradiated with a powerful excimer laser, which is tuned to a wavelength at which the absorption by the medium is as small as possible. Owing to the high parallelism of the laser beam, a steady, small concentration of active chlorine atoms can be generated in a very large volume and hence long chains are produced. At the same time, irradiation of the wall and hence the initiation of heterogeneous processes is to a large extent avoided. With laser radiation, faster conversion at lower temperatures can be achieved compared with other processes. Thus, both higher total conversions and reduced formation of side products are possible simultaneously. Like the thermally initiated process, the laser-induced production of vinyl chloride consumes energy. Therefore, besides the radiation intensity, the rate of heat transport from the walls into the gas is a limiting factor for the shortening of the reaction times. In addition, the interactions between the laser radiation and the reaction medium, which arise from the density and concentration gradients in flow reactors and can lead to undesired beam divergence and focusing,

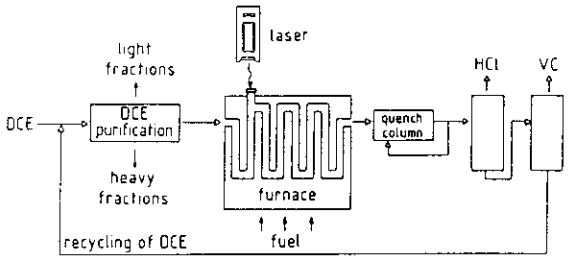

Fig. 23. Pilot plant for the production of vinyl chloride using an excimer laser.

have to be investigated in detail. A further problem in the industrial application of laser photolysis is the contamination of the windows through which the laser beam is admitted to the chemical reactor. One possibility is to flush the window with inert gas or cold DCE, which has a much lower absorption owing to the strong temperature dependence of the UV absorption of DCE. Under certain conditions, the laser itself can "burn" the windows clean by virtue of its high intensity. Compared with conventional photolysis setups, the required transmission surface is considerably smaller here. Overall, the use of high-power UV lasers in synthesis remains to be explored. Compared with the discharge lamps employed to date, the good spatial and spectral collimation of the laser radiation is particularly advantageous. This avoids too high radical concentrations in the vicinity of the light source and allows the required production of reactive radicals under the extreme conditions of pressure and temperature often encountered in large-scale industrial processes.

In the chlorination of 1,1-dichloroethane [Eq. (b)], hydrogen atoms can be replaced at two different positions. The desired α-substitution product, 1,1,1-trichloroethane, is employed as a metal degreaser in place of the more poisonous trichloroethylene. The maximum value of the α:β ratio is 9:1 using lasers compared with 1:1 for the classical thermal method and ca. 4:1 using a Hg lamp. The maximum selectivity is obtained when low-energy chlorine atoms, produced by the photolysis of ICl (from a mixture of iodine and chlorine) at 450 nm, are used as chain carriers.[49]

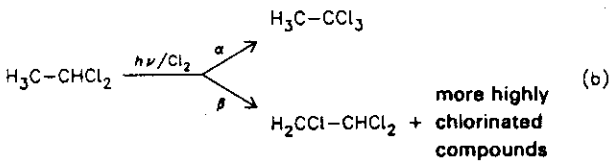

(b)

Ethylene can be produced from methane in the presence of chlorine at high pressure and temperatures around 900°C via a chain reaction [Eq. (c), (d)].[50] Under these

$$CH_4 + Cl_2 \longrightarrow CH_3Cl + HCl \quad (c)$$

$$2\,CH_3Cl \longrightarrow C_2H_4 + 2\,HCl \quad (d)$$

conditions, however, numerous undesired side products are formed. The methyl chloride produced in the first step [Eq. (c)] can alternatively be obtained in high quantum yield (ca. 10^4) at 200°C using a KrF laser (248 nm). The second step [Eq. (d)] can be initiated by an ArF laser (193 nm), although with a quantum yield of only 1.[51]

The dehydration of ethylbenzene to styrene [Eq. (e)] is catalyzed by OH initiator radicals obtained by photolysis (193 nm) of water vapor at 1 atm with an ArF laser; O_2 is added to prevent premature styrene polymerization.[52] Quantum yields of 10^5 at 500°C and 10^3 at 300°C were attained.

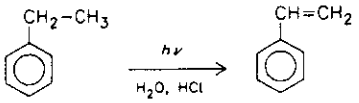

(e)

The photooxidation of cumene to cumene hydroperoxide [Eq. (f), (g)], a precursor of methylstyrene, is another example of a laser-induced chain reaction. In the thermal oxidation with air, numerous undesired side products are formed, whose amount can be reduced by lowering the temperature. By using photoinitiation, the reduction in reaction rate that occurs can be compensated for. At 351 nm (XeF laser), a quantum yield of approximately 500 is attained.[53] At shorter wavelengths (249 nm, KrF laser), the yield is reduced owing to photolysis of the product, cumene hydroperoxide.

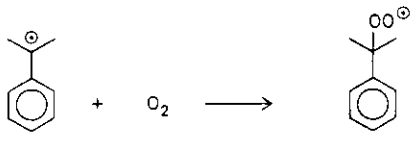

(f)

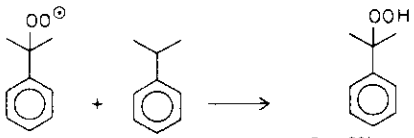

(g)

8 - 9%
(93% selectivity)

In the photooxidation of isobutane to *t*-butyl hydroperoxide, irradiation (351 nm) with a XeF laser also leads, on addition of chain carriers (HBr), to higher quantum yields, and higher selectivity is attained compared with thermal reactions.[54]

The ketene produced by rapid pyrolysis of acetone at 700°C can only be obtained in relatively small yields (ca. 20%) because of the rapid thermal decomposition that follows. By starting the chain reaction photochemically using a KrF laser (248 nm), higher conversions can be achieved. As in the production of VC, the quantum yield falls with increasing irradiation intensity.[55]

3.2. Laser-Induced Polymerization

Conventional light sources for photopolymerization in layers for reprographic technology as well as for curing synthetic insulating materials have already been applied in industry. Because only the initiator needs to be excited for photopolymerization, large quantum yields can, in principle, be achieved. As an example, the laser-induced, high-pressure polymerization of ethylene is considered in more detail. Numerous investigations have provided information on chemical and phase equilibria as well as kinetic parameters.[56] Thermally induced radical polymerization of ethylene has a number of disadvantages. Long induction periods result from the need to heat the monomer/initiator mixture. Also, the use of a multicomponent mixture (monomer/initiator/regulator) is usually necessary. Polymerization requires initiation by means of heat transfer, initially from the walls. The polymer coating so formed raises the heat transfer resistance of the reactor walls considerably. In the exothermic polymerization process, however, the removal of heat from the reactor is also an important parameter. Indeed, on exceeding a critical temperature, explosive decomposition of the monomers can occur. In contrast, providing the necessary initiation energy with the aid of laser radiation allows controlled and homogeneous initiation of the polymerization process. Figure 24 shows an experimental setup for investigating the UV laser-induced polymerization of ethylene at pressures up to 3000 bar and temperatures up to 300°C in the fluid phase. By means of quantitative infrared and near-infrared spectroscopy, the quantum yields and time course of the polymerization process as a function of pressure, temperature, and laser intensity can be studied directly over a wide range of conversions. Figure 25 shows the time course of the polymer formation as monitored by measuring the absorption of the second overtone of the C–H stretching vibration following initiation of the polymerization with a KrF laser (248 nm). As with the irradiation of DCE, one can work in a region of low absorption and hence achieve very large penetration depths in the starting material. However, the weak ethylene absorption at 248 nm (absorption cross section $\sigma = 2 \times 10^{-4}$ m^2 mol^{-1} at 100°C) is strongly influenced by impurities such as O_2. The absorption of the reaction product, polyethylene, at these wavelengths can be neglected. In the above experiments, quantum yields of 10^4 could be achieved and rate constants for the propagation and termination reactions of polymeriza-

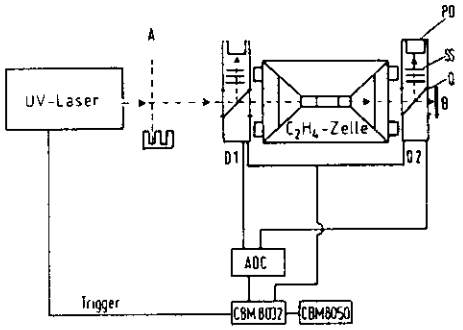

Fig. 24. Experimental setups for the investigation of the laser-induced high-pressure polymerization of C_2H_4. PD, photodiode; SS, scatterer; Q, quartz plate; B, pinhole; D1(2), detector 1(2); A, absorber; ADC, analog-digital converter.

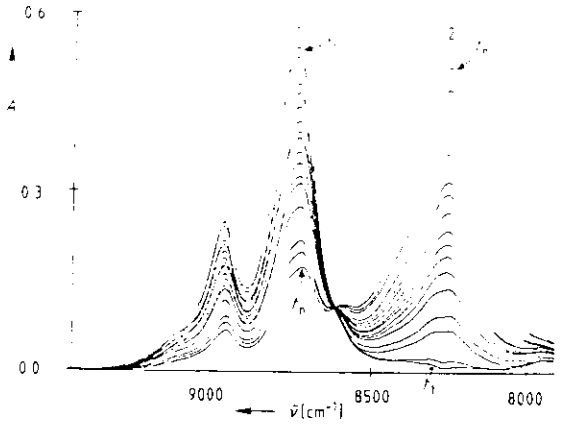

Fig. 25. Observation of polymer formation in C_2H_4 using the overtone spectrum of the CH stretching vibration after irradiation with a KrF laser. 1 = monomer band; 2 = polymer band; A = absorption, t_i = start, t_n = termination of spectral recording.

tion could be measured directly as a function of pressure and temperature.[56]

Polymerization by photochemical activation has also been achieved with infrared lasers[57] and continuously operating ion lasers; the laser-initiated copolymerization of cyclohexene oxide with maleic anhydride is two orders of magnitude more efficient than is the case for irradiation with conventional UV lamps.[58] On introducing a suitable photoinitiator, very rapid cross-linking in epoxy acrylate layers can be obtained by irradiation with an N_2 laser (337 nm). Up to 450 cross-link points are produced per absorbed photon. About 10^3 double bonds are polymerized for each initiator radical produced.[59] However, polymerization can also be initiated by laser photoionization. Cations can thereby be generated either from suitable, thermally stable salts[60] or by direct photoionization of the monomer via multiphoton processes.[61] The high temporal resolution feasible with laser photolysis also allows detailed investigations of the elementary processes involved in radical polymerization.[62] By introducing photochemically active catalysts, polymerization of acetylene and ethylene can be achieved in 3-μm-thick layers within the irradiation zone of an $Ar^{\oplus}$ ion laser (257.2 nm).[63] Interesting insight into the kinetics of the polymerization process can also be obtained using holographic techniques.[64, 65]

The irradiation of varnish coatings with excimer and dye lasers allows, even at very low intensities, very rapid polymerization without the use of solvents or heat. In this way, transparent coatings of 200-μm thickness and pigmented coatings of 20-μm thickness can be produced more than an order of magnitude faster than by the processes used previously.[66]

Laser-induced polymerization allows three-dimensional structures to be produced with high spatial resolution. To this end, two different laser beams are focused simultaneously on a point in a monomer solution, so that polymerization is initiated by two-photon excitation of the monomer or of the cross-linker. By controlling computationally the spatial position of the laser overlap zone of several micrometers diameter, one aims to produce complex, highly precise plastic prototypes and raw forms.[67]

3.3. Organic Photochemistry with Lasers

The photolytic ring opening of 7-dehydrocholesterol (7-DHC) (Fig. 26) to give vitamin D_3, via previtamin D_3 (P_3), has long been employed for the large-scale synthesis of vitamin D_3.[68] The three isomers lumisterol (L_3), tachysterol (T_3), and P_3 can be interconverted by irradiation with UV light, whereby the photostationary composition depends strongly on wavelength. Table 1 and Figure 26 show that the use of two laser wavelengths rather than irradiation with a Hg lamp leads to a considerable improvement in the yield of the desired vitamin D_3 precursor P_3.[69, 70] Irradiation with short UV light pulses in the picosecond range decreases the photolysis of P_3 and improves the ratio of P_3 to the undesired T_3 by another factor of 3.[71]

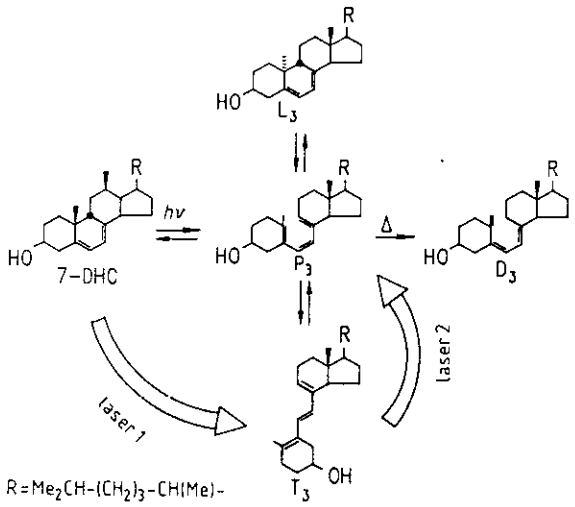

Fig. 26. Synthesis of vitamin D_3.

Table 1. Photostationary composition of the mixture upon irradiation of the vitamin D_3 precursor [69].

Light source	% 7-DHC	% T_3	% L_3	% P_3
Low-pressure Hg lamp	1.5	75.0	2.5	20.0
Medium-pressure Hg lamp	3.4	26.0	17.0	53.0
KrF laser (248 nm)	2.9	71.0	—	26.0
XeCl laser (308 nm)	13.0	3.4	42.0	35.0
KrF + N_2 laser (334 nm)	0.1	11.0	9.0	80.0

The results of the laser experiments allow improvements in the conventional photochemical process: namely, the KrF laser (248 nm) and the N_2 laser are replaced by a low-pressure Hg lamp (254 nm) and a medium-pressure Hg lamp equipped with a suitable filter, respectively. In the production of special vitamin D_3 metabolites for medical diagnostics, an increase in yield by a factor 5 is achieved by the use of lasers.[72]

Peroxides, which are produced from azoalkanes, are important intermediates in the synthesis of the beetle attractant pheromone frontalin.[73] Alone in North America, the beetles *Dendroctonus brevicomis* and *D. frontalis* cause more than a billion dollars worth of damage to wood annually. Frontalin (Fig. 27) can be produced from the azoalkane **1** via the endoperoxide **2**. The 364-nm line of the $Ar^{\oplus}$ laser is particularly suitable for this synthesis, since this

wavelength is absorbed sufficiently by the sensitizer benzophenone but not by the azoalkane 1. In contrast, direct light absorption by the azoalkane results in loss of N_2 and formation of a singlet diradical which undergoes C–C bond closure to give an undesired product.

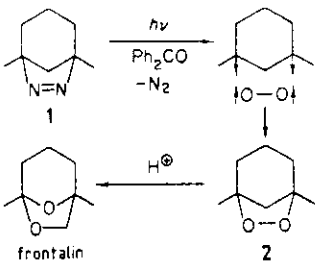

Fig. 27. Synthesis of frontalin. Direct photolysis of 1 results in the formation of a triplet diradical which reacts with O_2.

Similarly, certain azoalkanes can be converted into endoperoxides by laser photolysis followed by scavenging of the resulting diradicals with O_2. From those endoperoxides, substances for preventing (prostacyclins) or promoting (thromboxane) blood clotting can also be produced.[73] The photodecomposition of vitamin K, 3, which leads to termination of respiration in living cells, can be traced back to the reaction of the preoxetane diradicals 4 with O_2.[73] By using high O_2 partial pressures (> 10 bar) and photosensitization with benzophenone, the diradicals 5 and 6 can be scavenged in high yields as the corresponding peroxides.[74]

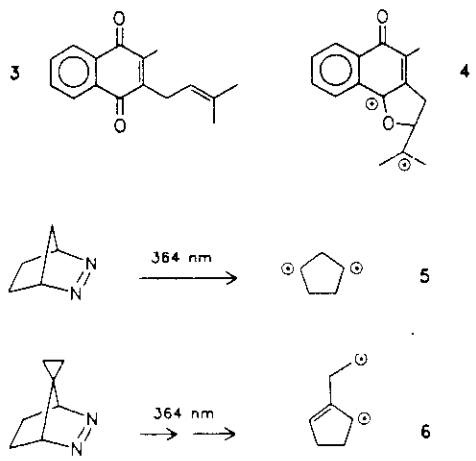

With high-power pulsed lasers, sufficiently high concentrations of radicals can be produced for direct spectrally and temporally resolved detection.[75] Also, higher triplet and singlet states can be reached by successive absorption of laser pulses in the nanosecond and picosecond range (Fig. 28).[76] For a triplet-state lifetime of 10^{-4} to 10^{-7} s, laser intensities of 10^4–10^7 W cm^{-2} are sufficient and are easily attainable using excimer lasers at pulse lengths around 10^{-8} s. In this way, the quantum yield of the photocyclization of carvone 7 to carvone camphor 8 [Eq. (h)] in ethanol can be increased 70-fold compared with the single-

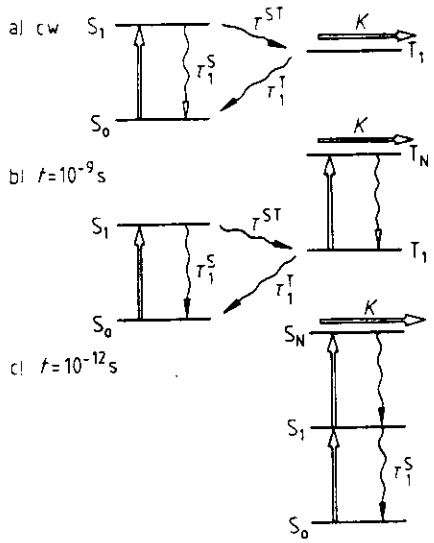

Fig. 28. Reaction possibilities of polyatomic molecules after single-photon and multiphoton excitation by laser pulses of differing duration. a) The relatively small intensity of the continuous (CW) laser leads to excitation only of the S_1 or T_1 state. b) With laser intensities of 10^4–10^7 W cm^{-2} and pulse lengths in the nanosecond range, higher states can also be reached by successive absorption of photons. c) The direct excitation into higher singlet states requires intensities of 10^9–10^{10} W cm^{-2} and pulse lengths of 10^{-12} s. Molecules in higher singlet or triplet states can undergo new reactions (K). τ_1^S, τ_1^T, and τ^{ST} are the characteristic lifetimes of the S_1 state, the T_1 state, and the transition from the S_1 to the T_1 state.

photon excitation.[77] The direct excitation to give higher singlet states requires laser pulses of around 10^{-12} s, since, for the intensities of 10^9–10^{10} W cm^{-2} required for pulses of 10^{-8} s, the damage threshold of the condensed phase is considerably exceeded. Excitation of maleic acid with pi-

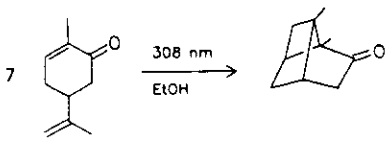

(h)

Fo. 5

Angew. Chem. A 601 Fo. 4 + 5 WERK FACHA A60102

cosecond pulses at 265 nm results not only in photodimerization, but, with increasing intensity, also in addition of water to the double bond.[76] Here, the direct cleavage of water by multiphoton excitation apparently plays an important role.[79] The use of ultrashort light pulses of high intensity could open interesting new approaches to the photochemistry of energy-rich double bonds: for example, in the development of optical switches, the construction of organic molecules for energy and information storage, and the synthesis of active substances. Still little used is the selective production of enantiomers by photolysis with polarized light, already described in the 1930s by *W. Kuhn* et al.[80]

The intensive efforts to apply organic glasses and polymers to optical storage of data[81] have already been reported in detail.[65,82] More recently, both for inorganic[83] and for organic[84] materials, interesting results have been achieved by "multicolor" photoionization (simultaneous irradiation with photons of various wavelengths).

3.4. Separation of Isotopes with Lasers

The high frequency sharpness of the electromagnetic radiation possible with the laser has given new impetus to investigations of the photochemical separation of isotopes, which was first attempted over half a century ago.[85] A specific isotope of an element (either in the elemental state or in a molecule) is excited selectively by narrow-band laser light and converted into an ion, isomer, or dissociation or reaction product that can be more readily separated chemically or physically (Fig. 29). The focus of interest was initially the uranium isotope ^{235}U.[86] The most developed process for this so far, AVLIS (*a*tomic *v*apor *l*aser *i*sotope *s*eparation), employs the selective multiphoton ionization of uranium atoms (Fig. 29a) with dye lasers, pumped by powerful copper vapor lasers with high repetition frequency (10 kHz).[87] Besides uranium and plutonium, numerous other elements can be isotope-selectively enriched by this method.[88]

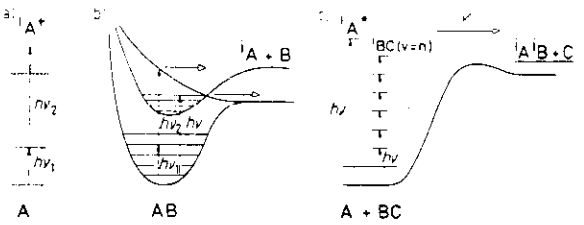

Fig. 29. Possibilities for photochemical separation of isotopes with the laser. 'A represents a particular isotope of the element A. For details, see text.

Following the observation of isotope-selective, infrared multiphoton dissociation of SF_6 with the aid of CO_2 lasers,[22] analogous experiments were performed with UF_6. The radiation required for excitation of the fundamental vibrations of UF_6 at 16 μm can be obtained by rotational Raman scattering of CO_2 laser radiation on para-hydrogen.[89] However, the UF_6 gas beam has to be strongly cooled to obtain the necessary differences in absorption between $^{238}UF_6$ and $^{235}UF_6$. By further selective vibrational excitation of UF_6, clear differences are obtained in the UV absorption spectra[90] of $^{238}UF_6$ and $^{235}UF_6$, which can be used for the isotope-selective dissociation shown in Figure 29b. The laser powers at 308 nm required for industrial application are in the 100-kW range.[91] Besides UF_6, other uranium compounds, such as $UO_2(OCH_3)_6$[92] and uranium complexes[93] were investigated. The technique was also applied successfully for the enrichment of plutonium isotopes by selective excitation of PuF_6.[94] In nuclear power reactors, zirconium is used as a containment material for fuel rods. Isotope separation is of interest since ^{91}Zr has a neutron-capture cross section more than an order of magnitude larger than the other isotopes. Indeed, the selective ionization of ^{91}Zr was reported recently.[95] Because the economic use of nuclear fission is developing more slowly and with more difficulty than was originally assumed, the requirement for additional capacity for isotope separation of uranium is smaller than predicted. This is also true for deuterium,[96] which is required for reactors using natural uranium. Tritium can be enriched (e.g., for experiments in controlled nuclear fusion) by multiphoton excitation of $^3HCCl_3$[97] and $^3HCF_3$[98] with an IR laser.

The isotope-selective dissociation by one-photon excitation (Fig. 29b) can also be achieved by selective excitation of predissociative states, as for isotopes of carbon in formaldehyde.[99] ^{13}C-labeled compounds can be used in medical diagnostics, for example, in metabolic investigations in place of radioactive ^{14}C-labeled compounds, and in NMR tomography. An annual requirement of several hundred kilograms of ^{13}C is to be expected. An industrially relatively well developed process for laser-induced production of carbon isotopes is presented schematically in Figure 30.[100] Laser-induced multiphoton dissociation (Fig. 29c) of Freon 22 (CF_2HCl) results in the formation of C_2F_4, from which ^{13}C-enriched CF_2HCl can be obtained by thermal addition of HCl.[101] The cost of the CO_2-laser photons required for this process can be reduced still further by employing a continuous-discharge CO_2 laser.[102] Enrichment of ^{13}C-isotopes via multiphoton dissociation of CF_3Br[103] is more expensive, because of the considerably higher cost of the starting material. Isotopes can also be enriched by selective excitation of bimolecular exchange[34,104] or addition reactions.[105]

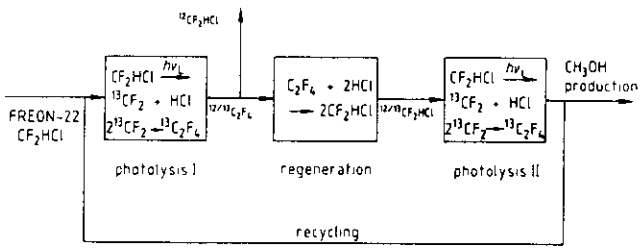

Fig. 30. Production of ^{13}C-enriched compounds by multiphoton dissociation of Freon-22. Photolysis I ($\lambda = 9.5$ μm) leads to a mixture of $^{12/13}C_2F_4$ and $^{13}CF_2HCl$. After separation of $^{12}CF_2HCl$, the remaining $^{12/13}C_2F_4$ is reconverted into $^{12/13}CF_2HCl$ and further enriched with the ^{13}C-isotope by photolysis II ($\lambda = 9.5$ μm).

3.5. Photochemical Purification with Lasers

The selective photochemical removal of impurities with lasers is exemplified by the purification of gaseous SiH_4 (the starting material for the preparation of pure silicon for semiconductor production) from compounds such as AsH_3, PH_3, and B_2H_6, which are difficult to remove chemically. Contamination of such p- and n-charge carriers, even at a ratio of $1:10^9$, can negatively influence the functioning of integrated circuits. Whereas in conventional methods the entire material is subjected to the purification process, the laser acts only on the impurities. Thus, laser irradiation at $\lambda = 193$ nm is absorbed four orders of magnitude more strongly by PH_3 and by AsH_3 and two orders of magnitude more strongly by B_2H_6 than by SiH_4. For an impurity of 1%, more than 99% of the AsH_3 and 40% of the PH_3 and B_2H_6, but only 1% of the SiH_4 is photolyzed.[106] The end products of this photolysis are readily separable solid polymers or gaseous compounds. Laboratory experiments show that the purification process even proceeds ef-

ficiently at atmospheric pressure, so that, for impurities of several ppm, typical absorption cross sections of 10^{-17} cm^2 and reactor lengths of several meters, more than 50% of the laser light is absorbed. Extremely high-purity silane is important for the economic production of electricity from sunlight, since the efficiency of silicon solar cells depends strongly on the impurities present. Further examples of efficient purification of gases are the separation of $COCl_2$ from BCl_3[107] and of CCl_4 from $AsCl_3$[108] and the destruction of dioxin.[109]

Lanthanoids and actinoids can be efficiently separated and purified by exciting the narrow absorption bands of their compounds in the visible and UV.[110] The excitation is still selective even for higher absorber densities in the liquid phase. The new oxidation states formed by the photoredox processes enable the compounds to be readily separated. Figure 31 shows the separation of europium [Eq. (i)] as an example, whereby the hydroxyl radical has to be scavenged, e.g., by isopropanol, to avoid the reverse reaction. The quantum yield for $Eu^{3\oplus}$ photoreduction at

$$Eu^{3\oplus} + H_2O \xrightarrow{193\ nm} Eu^{2\oplus} + H^{\oplus} + OH^{\odot} \quad (i)$$

$$Eu^{2\oplus} + SO_4^{2\ominus} \longrightarrow EuSO_4\downarrow$$

193 nm was given as 5% at 90% conversion, whereby up to a three-hundred-fold enrichment of europium was measured in the precipitate after irradiation of binary europium/lanthanoid mixtures. H_2S in CO/H_2 synthesis gas was photolyzed selectively with an ArF laser and the sulfur released was removed by adsorption on a metal surface.[111] In this way, sulfur impurities could be reduced from 10 ppm to 1 ppm. A spectroscopic selectivity (excitation only of H_2S in the synthesis gas) of 10^7 was measured in the wavelength range 210–220 nm. Quantum yields (H_2S molecules removed per absorbed photon) of 0.4 (1 atm) to 1.0 (10 torr) were achieved. In particular, the use of a laser is interesting for the removal of "fine impurities" (< 1 ppmH_2S), since catalysts based on copper (e.g., those used for production of methanol from synthesis gas) have lifetimes of about one year if the H_2S impurities in the CO/H_2 mixture can be reduced to less than 1 ppm.

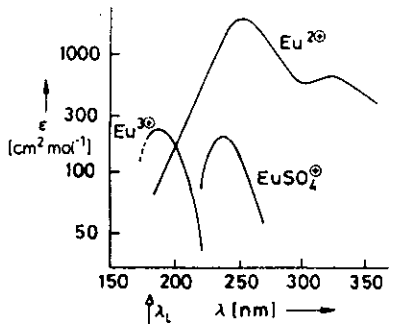

Fig. 31. Laser-induced separation of lanthanoids. The absorption spectra of europium in various oxidation states show that the $Eu^{3\oplus}$ ions can be selectively reduced in the liquid phase with the aid of an ArF excimer laser (λ_L = 193 nm). The $Eu^{2\oplus}$ ions formed are precipitated as $EuSO_4$ after reaction with sulfate ions.

3.6. Synthesis of Defined Solids and Catalysts with Lasers

Pyrolysis of gas mixtures with laser radiation can be used to produce catalytically active solids of variable composition (Fig. 32). After complete mixing of the gaseous starting materials and their rapid heating in the laser beam,

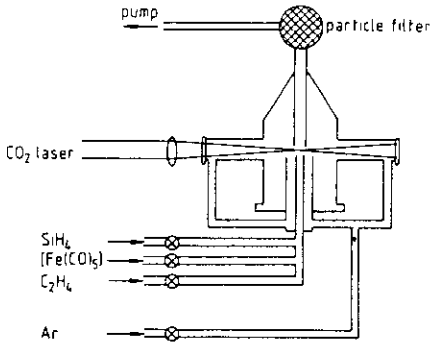

Fig. 32. Synthesis of Fe/Si/C catalysts by CO_2 laser pyrolysis of gaseous starting materials. By varying the partial pressures of the components and the laser intensities, catalysts with varying properties can be produced.

very small solid particles with homogeneous structure and large surface area are obtained. Figure 33 shows the yield of alkanes and alkenes obtained from the Fischer–Tropsch synthesis with laser-synthesized Fe/Si/C catalysts. Whereas with saturated hydrocarbons mainly methane is formed, with olefins considerably longer chains are obtained. By optimizing the composition of the laser-synthesized catalysts, higher selectivity and preferential formation of the valuable light olefins (C_2–C_4) can be achieved.[112] By a similar process to that described in Figure 32, powders of defined composition can be obtained for the production of specialty ceramics.[113] Irradiation of $[Fe(CO)_5/SiH_4$,[114] NH_3/SiH_4,[115] $(Me_3Si)_2NH$,[116] or $SiH_4/NH_3/CH_4$[117] gas mixtures with a CO_2 laser leads to particularly fine, pure, spherical, relatively non-clumping, and almost identically sized Si/Fe, Si_3N_4, and Si/C/N grains for the production of special ceramics.

Metal carbonyl catalysts can be UV-photoactivated instead of thermally activated. Active centers are formed by cleavage of one or more CO ligands, often resulting in ca-

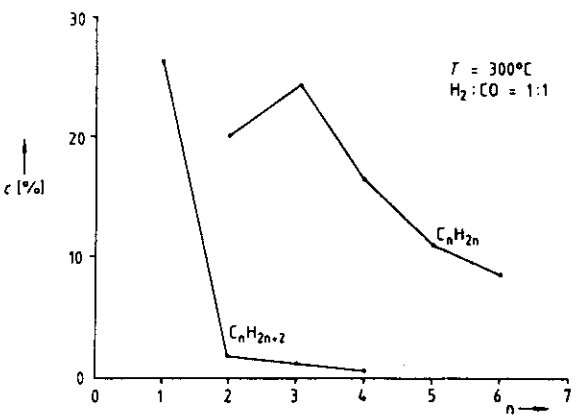

Fig. 33. Fischer–Tropsch synthesis with laser-produced Fe/Si/C catalysts. n = number of C atoms; c = amount of product in %.

talytic activity even at room temperature. Besides polymerization (Section 3.2), the isomerization and hydration of alkenes with $[Fe(CO)_5]$ catalysts[115,119] and the silylation of alkenes and aldehydes[118,130] with $[Co_4(CO)_{12}]$ catalysts upon irradiation with a XeF laser or a frequency-doubled Nd-YAG laser have been investigated. For the isomerization of 1-pentene, quantum yields of 10^3 and "turn-over" rates (quantum yield per average lifetime of the catalyst) of 4×10^3 s^{-1} at 50% conversion of 1-pentene can be achieved. Broad-band light sources such as flash lamps lead more readily to direct photolysis and to undesired side products.

Metallic glasses having unusual compositions and properties and other metastable phases can be produced by irradiation with intense laser pulses. Short laser pulses lead here to extremely rapid heating and melting, followed by very rapid cooling and solidification. Cooling rates of up to 10^{12} K s^{-1} have been obtained for alloy films after heating by means of picosecond laser pulses.[121]

3.7. Laser-Induced Deposition of Materials on Surfaces

In conventional, thermally induced deposition of materials from the gas phase (*c*hemical *v*apor *d*eposition, CVD), relatively high temperatures (600–900°C) are required. The temperature can be reduced to 350–450°C by employing electrical discharges in plasma CVD. However, undesired species can be formed in wall reactions and interfere with the process, and radiation damage can be induced in the deposited films; moreover, in order to ensure the stability of the discharge, only a restricted range of pressures is available and the reaction volume can only be controlled to a very limited extent. The LICVD method (*l*aser-*i*nduced *c*hemical *v*apor *d*eposition) for controlled deposition of selected species offers many advantages: control of the irradiation area from μm^2 to cm^2 and of the irradiation time from 10^{-14} s to continuous operation, no wall effects, and independent control of the substrate temperature for production of layers with extremely high purities.

Figure 34 shows schematically three possibilities for the LICVD method.[122] In the pyrolytic process (I), the laser light is generally not absorbed by the reaction gas, but is used instead to produce strong localized heating at the substrate surface. Because of the strong temperature gradient formed, the material is deposited in a narrowly defined region, so that transport from the gas phase can occur from various directions. The pyrolytic method can be applied over a wide range of pressures and allows deposition rates on the order of 1 to 10^2 $\mu m\ s^{-1}$, a factor of 10^2 to 10^4 higher than with a conventional CVD process.[123] In process II, a better directed and more homogeneous beam of the material to be deposited is obtained than in the ion vaporization technique otherwise generally employed.[124] In the photolytic process (III), selective excitation of dissociating states is employed. The products of laser dissociation can either be condensed directly on the surface or allowed to react chemically with other species present in the surface layer. As shown in Figure 35 III, the laser can also be focused directly on the surface and moved over it.

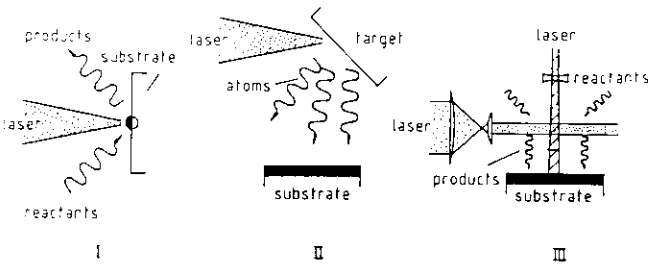

Fig. 34. Possibilities for the photochemical deposition of materials from the gas phase by means of IR or UV lasers. For details, see text.

Frequency-doubled $Ar^{\oplus}$ lasers ($\lambda = 257$ nm) can be used to deposit Cd from $Cd(CH_3)_2$,[125] Zn from $Zn(CH_3)_2$,[126] and Ni from $[Ni(CO)_4]$.[127] Because of the nonlinearity of the grain-formation process, spatial resolution of 0.2 to 0.5 μm is obtained. In conjunction with computer control of the laser beam, it is therefore possible to "draw" complex electronic circuits directly onto a substrate.[128] Besides metallic conducting layers, insulators and semiconductor layers can also be deposited. In addition to continuously operating ion lasers, CO_2 and UV-excimer lasers can be employed, which permit the production of large-surface-area, thin layers, e.g., amorphous Si layers for the production of cheap solar cells.[129] The rate of deposition can be increased considerably by the participation of the photoelectrons produced by the UV excimer laser.[130] Information on the primary processes occurring on applying the radiation of a UV-excimer laser for the deposition of metals from organometallic compounds (MOCVD) can be obtained using multiphoton mass spectrometry with time-of-flight analysis. This technique allows the production of an entire mass spectrum with high sensitivity by using a single laser pulse.[131] The species involved can be identified from both their absorption spectra and their masses. In this way, the formation of tellurium atoms and dimers upon photolysis of $Te_2(CH_3)_2$ at two different laser wavelengths, the energy states of the Te atoms formed, and the energy distribution within the molecular fragments can be determined directly. Use of ultrashort light pulses appreciably facilitates the detection of unstable parent ions.[132] Further, the deposition and dissolution rate of metals at liquid/solid boundaries can be increased considerably ($> 10^3$) by the use of laser radiation. The laser beam is directed onto the cathode in an electrolyte solution and the laser wavelength chosen so that the electrolyte absorbs as little as possible.[133,134] Metal deposition without electric current is also feasible.

4. Ablation and Processing of Materials with Lasers

Two types of material processing with lasers can be distinguished: thermal, nonreactive processing and chemical processing. In thermal processing, the sample is heated locally and brought to melting and evaporation. Welds and cuts can be made on the sample. This method is applied in a modified form to anneal defects on surfaces, to recrystallize, to harden materials, or to alloy locally. In chemical processing, chemical reactions are initiated by the laser radiation.

4.1. Processing of Polymer and Semiconductor Materials

In principle, any laser with sufficient power density is suitable for processing of polymer materials and substrates for microchips. Recently, however, several significant advantages of UV lasers have become apparent,[134] particularly when microscopically fine and precise work with clean edges is required. These types of requirements arise especially in the production of chips of very high information density (microlithography), but also in "microwriting" on polymer materials and in micromanipulation of biological objects. A significant advantage of UV light is that at wavelengths below ca. 350 nm the energy of single photons is sufficient to break chemical bonds. In contrast to IR lasers, whose radiation can penetrate more deeply and excite vibrations in polymer molecules, leading to thermal decay, the use of UV lasers results in cleavage of bonds where the photon density is highest, i.e., on the surface. This leads predominantly to monomer fragments and very clean ablation edges.[135] By laser decomposition of halogen compounds adsorbed on surfaces, fine patterns can be etched in semiconductors, glasses, metals, ceramics, and other materials.[136]

The following processes occur in etching:

Photodissociation	CH_3Br	$\longrightarrow CH_3^{\odot} + Br^{\odot}$	
Chemisorption	n(Br)	$\longrightarrow$ (nBr):(GaAs)	$\Delta H < 0$
Surface erosion	(nBr):(GaAs)	$\longrightarrow GaBr_n + As$	
Evaporation	GaBr (solid)	$\longrightarrow$ gallium bromide (g)	

Free halogen atoms are removed from the gas phase by radical scavengers, so that the etching process occurs only in the direct vicinity of the laser beam. The method is also applicable to liquid/solid boundaries.

5. Application of Lasers in Medicine

Most of the laser applications described below are not yet accepted in routine clinical practice. The application of the laser in surgery offers a number of advantages: stypsis, precise work, reduction in the number of instruments required, contact-free tissue ablation, asepsis, minimal damage to the surrounding tissue.[137] In respiratory tract or gynecological operations, the laser light can be led directly to the site of operation via light guides.

For laser light to interact with tissue, it must first be absorbed. Several simple observations can be made:

1. The interaction with IR radiation is best described in terms of absorption by water. The interaction is predominantly thermal in nature.
2. The absorption properties with respect to visible light are determined by the pigmentation of the tissue in question.
3. The further one goes into the UV, the more important photochemical effects become. At wavelengths below 200 nm, photoablation occurs almost exclusively. Here, the interaction of light with polymers (Section 4.1) can serve as a model.

This overview says nothing about the influence of power density on the interaction of laser light with tissues. Table 2 shows the variety of interactions possible and how they can be applied in medicine. The data in Table 2 are collected mostly from ref. [137, 138]. Table 3 gives an overview of the lasers used in medicine and their applications, which will be illustrated below with no attempt at completeness.

The aim of *angioplasty* with lasers is to open sclerotic blood vessels.[140] The use of lasers operating in the visible or infrared, however, results in carbonized edges and bubblelike lesions in the vessel tissues, which remain after removal of the stenosis.[141] Thrombocytes attach themselves to such edges and are the starting point for a new stenosis. Very recently, it was shown that these problems do not arise when ArF excimer lasers are used.[142] The edges of the recanalized tissue are smooth (Fig. 35).[143]

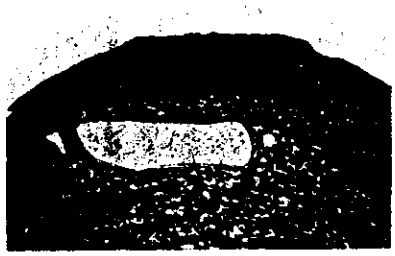

Fig. 35. Histological section through aorta tissue that has been recanalized using an ArF laser. Enlargement ca. 100-fold; laser power ca. 50 J cm^{-2} [143].

Table 2. Medically useful interactions of light and matter.

Power density	Type of interaction	Mechanism	Application
mW/cm^2	Biostimulation [139]	Influencing certain parts of metabolism	Healing of inflammations and wounds
kW/cm^2	Coagulation	Denaturation and resulting clotting of proteins, etc., at local temperatures of 40–80 °C	"Glueing" of tissue parts; clotting of bleeding
MW/cm^2	Evaporation	Water evaporates (partly explosively) from the tissue; breakdown of tissue structure	Cutting of tissues analogous to the surgical knife but contact-free.
GW/cm^2	Photoablation Photodisruption	Individual bonds are broken	Cold evaporation of tissue parts
TW/cm^2	Formation of microplasms	Molecules are ionized so that electron avalanches occur	Destruction of "hard" materials such as gallstones

Table 3. Possibilities for application of material processing in medicine

Laser type	Working wavelength [nm]	Presumed nature of interaction with tissue	Penetration depth into the skin	Main use following interaction [a]					Areas of medical application [b]					
				A	B	C	D	E	U	V	W	X	Y	Z
ArF excimer	193	photolysis, cold evaporation	Surface				×	×	×					
KrF excimer	248		Very small			(×)	×	×	×					
XeCl excimer	308		Small			×	×	×	×					
Kr^+ ion	407		Deep	×	×	×				×				
Ar^+ ion	516		Very deep	×	×	×				×	×	×	×	
Nd-YAG, frequency-doubled	532		Very deep		×	×	(×)			×				
He-Ne	620		Very deep	×						×				×
Semiconductor	780-1200		Deep	×										×
Nd-YAG	1064		Deep		×				×		×	×	×	
Er-YAG	2936	thermal	Small										×	
CO_2	10000	thermal	Small			×			×		×	×		

[a] A = biostimulation; B = coagulation; C = evaporation, cutting; D = photoablation, photodisruption; E = formation of microplasms. [b] U = angioplasty, V = photodynamic therapy, W = urology - gynecology, X = gastroenterology, Y = ophthalmology, Z = dental medicine.

In *tumor therapy with lasers*, two methods are being explored. One attempts to coagulate tumors directly[144] and the other uses the laser for photodynamic therapy (PDT).[145] In PDT, dyes are employed that absorb light of a particular wavelength preferentially and are either incorporated selectively in the tumor tissue or are more slowly degraded by the tumor tissue. An example is provided by the hematoporphyrin derivatives (HpD), which are incorporated selectively by the vessel tissue of tumors. If the tumor is irradiated with a red laser (e.g., He-Ne laser), the HpD-labeled tumor tissue absorbs selectively. HpD is decomposed photolytically, so that oxygen radicals are formed, which as strong cytotoxins interfere with the blood vascular system of the tumor and hence cut off its supply of nutrients. Other dyes, such as phthalocyanines, are incorporated preferentially in the mitochondria of cancer cells and after laser irradiation interfere with the metabolism of these cells.

Numerous tumors can be temporarily degraded by use of PDT. Nevertheless, baring individual exceptions, cancers cannot be cured in this way, since the metastases are not treatable and the effects of PDT on various tumors vary greatly.[146]

PDT is still being investigated to some extent in animal experiments for the treatment of bladder tumors,[147] breast cancer,[148] gynecological tumors,[149] intestinal cancer[150] and lung tumors. The selectivity for certain tumors might be increased by coupling monoclonal antibodies to HpD.[151]

A very attractive application of lasers in *gastroenterology* could be in the destruction of gallstones. In contrast to kidney stones, 90% of which can be destroyed by a lithotripter without an operation, gall stones are insensitive to fluid shock waves. In contrast, laser pulses of high power density destroy gall stones, probably after forming microplasms which break the stones from within. For this type of application, the excimer laser is probably the most suitable.

All *lasers* that are suitable for coagulation of tissue can also be applied to *stop stomach hemorrhages* by thermally clotting the blood. In contrast to drug therapies to stop hemorrhages, one can work very well locally with the laser and thereby avoid irritating the neighboring tissue.

In *neurosurgery*, lasers have long been used to treat tumors in the brain.[152] In particular, the possibility of precise, contact-free operation is made use of since in brain surgery, even more than for other parts of the body, it is important to protect healthy neighboring tissue. Most recently, first results on the application of lasers in microsurgery were reported.[153] Here, the coagulating action of a focused laser was used to reconnect interrupted nerve connections very precisely.

In *dermatology*, hemorrhages that form in the skin by perforation of capillary vessels can be treated by the green light of the Ar^+ laser[154] and the frequency-doubled Nd-YAG laser. In this way, blood clots are destroyed and simultaneously capillary vessels are closed. Less specific is work with the CO_2 laser, whose thermal effect is used, for example, to remove warts or tatoos.[155]

The development of laser treatment methods in ophthalmology is the most advanced and illustrates clearly how completely different results can be achieved by choosing a suitable laser wavelength. With an Nd-YAG laser, one can reach areas just behind the eye lens on account of the shallow penetration depth of IR light. Membranes can therefore be opened, through which intraocular overpressure

can be released. The green light of the Ar^+ laser,[156] the frequency-doubled light of the Nd-YAG laser,[157] or the blue light of the Kr^+ laser can be used to reach the fundus of the eye, the retina, through the transparent eye lens and the transparent vitreous humor, for example to "weld" (coagulate) detached areas of the retina. For corrections of curvature defects of the cornea, on the other hand, wavelengths that are absorbed by the cornea, such as those of excimer laser light, are needed.[158] With the aid of cylindrical lenses, excimer laser pulses are imaged to a streak-formed cross section, which is used to change the radius of curvature in the desired manner.

In treatment of opthalmic disorders, another important advantage of the laser is apparent: often, the laser, which is required for material processing, i.e., operational tasks, can be employed by means of a suitable regulation technique for diagnosis and analysis of the operation results. This not only reduces the number of instruments required for the operation but but also reduces the irritation to which the eye is exposed.[159]

6. Summary and Outlook

Twenty-five years after its discovery, the laser is irreplaceable in many areas of basic chemical research. The use of lasers provides a direct approach to the investigation of the molecular details of chemical reactions. The results can be compared directly with predictions based on quantum-mechanical calculations. The data so obtained on reaction cross sections and rate constants of elementary chemical processes can be used as a basis for detailed mathematical modeling of chemical reactions, which in the future will have the same significance that tables of thermodynamic values have at present. Investigations with lasers will increasingly provide information on numerous kinetic processes in gases, liquids,[160, 161] and solids as well as in biological systems. A significant breakthrough in the investigation of changes in molecular structures in the course of chemical and biological processes is to be expected from the extension of the laser principle to the X-ray region. Although stimulated emission has been observed down to wavelengths of 21 nm, for the region of several nm considerable difficulties still have to be overcome,[6b, 161] because extremely high pumping efficiencies are required owing to the short lifetimes of excited states in the X-ray region.

Although the cost of laser photons is at present markedly above that of photons from conventional light sources, photochemical synthesis with lasers can afford a number of interesting results. In particular, the laser-photochemical production of thin layers of metal, insulators, and semi- and superconductors will acquire increasing technological importance, not only for newer processing techniques for semiconductor components and circuits, but also particularly for the development of integrated sensors for controlling automated finishing processes. The application of lasers for the production of larger quantities of isotopically pure compounds, specific pharmaceuticals, initiation of chain reactions in the production of monomers or the polymerization of coating layers, and the production of powders for ceramics and catalytically active material will depend on how far the costs of laser photons can be further reduced and whether lasers with higher powers and lifetimes become available. For some technical applications, such as laser printers and material processing using CO_2 lasers, these requirements have already been met. For excimer lasers, systems with powers in the kW range will be realized in the near future. It is at present hard to estimate how far new laser principles, such as the free electron laser (FEL), will allow high powers and efficiencies in a wide range of wavelengths from the infrared to the ultraviolet to be attained. So far, FEL systems have only been operated in the infrared and visible spectral regions, whereby extreme demands on the quality of the electron beam are made.

It is assumed that, besides the production of chemical products and the processing of technical materials, high-power lasers will be of particular interest for applications in medicine. A significant advantage of the laser is that one can penetrate inside the body using light guides. However, for this purpose, very high laser powers often have to be transported if specific photochemical effects, and not just thermal effects, are desired in the processing of biological material. Suitable optical materials still need to be developed for this purpose.

We thank numerous colleagues for sending material for the review and Dr. K. O. Greulich (Heidelberg) for compiling the section on the application of lasers in medicine. Financial support for our work was received from the Fonds der Chemischen Industrie, the Deutsche Forschungsgemeinschaft, the Stiftung Volkswagenwerk, and the Bundesministerium für Forschung und Technologie.

Received: June 27, 1986 [A 601 IE]
German version: *Angew. Chem. 99* (1987) 38
Translated by Dr. *Penelope Monkhouse*, Heidelberg

[1] A. Einstein, *Phys. Z. 18* (1917) 121.
[2] J. P. Gordon, C. H. Townes, *Phys. Rev. 99* (1955) 1264.
[3] T. H. Maiman, *Nature (London) 187* (1960) 493; P. J. Collins, D. F. Nelson, A. L. Schawlow, W. Bond, C. G. B. Garrett, W. Kaiser, *Phys. Rev. Lett. 5* (1960) 303.
[4] J. Wolfrum, *Nachr. Akad. Wiss. Göttingen Math. Phys. Kl. 2 1973*, No. 5.
[5] F. P. Schäfer, W. Schmidt, J. Volze, *Appl. Phys. Lett. 9* (1966) 306; P. P. Sorokin, J. R. Lankard, *IBM J. Res. Dev. 10* (1966) 162.
[6] a) W. Demtröder, *Laser Spectroscopy Springer Ser. Chem. Phys. 5* (1981); b) F. P. Schäfer, *Phys. Bl. 42* (1986) 283.
[7] D. R. Crosley (Ed.): *Laser Probes for Combustion Chemistry (ACS Symp. Ser. 134)*, Washington 1980.
[8] H. A. Schwarz, R. R. Williams, Jr., W. H. Hamill, *J. Am. Chem. Soc. 74* (1952) 6007; R. M. Martin, J. E. Willard, *J. Chem. Phys. 40* (1964) 3007.
[9] J. Warnatz, *Ber. Bunsenges. Phys. Chem. 87* (1983) 1008; J. Wolfrum, *XXth Symp. (Int.) Combust.* (The Combustion Institute, 1985) 64.
[10] K. Kleinermanns, J. Wolfrum, *J. Chem. Phys. 80* (1984) 1446.
[11] C. F. Melius, R. J. Blint, *Chem. Phys. Lett. 64* (1979) 183.
[12] K. Kleinermanns, R. Schinke, *J. Chem. Phys. 80* (1984) 1440.
[13] T. Just, P. Frank, *Ber. Bunsenges. Phys. Chem. 89* (1985) 1981.
[14] C. Cobos, H. Hippler, J. Troe, *J. Phys. Chem. 89* (1985) 342.
[15] K. Kleinermanns, E. Linnebach, *J. Chem. Phys. 82* (1985) 5012.
[16] K. Kleinermanns, E. Linnebach, *Appl. Phys. B 36* (1985) 203.
[17] a) H. H. Dispert, M. W. Geis, P. R. Brooks, *J. Chem. Phys. 70* (1979) 5317; b) Z. Karny, R. C. Estler, R. N. Zare, *ibid. 69* (1978) 5199; c) C. Man, R. C. Estler, *ibid. 75* (1981) 2779; d) F. Heismann, H. J. Loesch, *Chem. Phys. 64* (1978) 5199; e) M. Hoffmeister, L. Potthast, H. J. Loesch, *ibid. 78* (1983) 4376.
[18] R. Altkorn, F. E. Bartoszek, J. Dehaven, G. Hancock, D. S. Perry, R. N. Zare, *Chem. Phys. Lett. 98* (1983) 212.

[19] a) P. Andresen, A. C. Luntz, *J. Chem. Phys. 72* (1980) 5842; b) K. Kleinermanns, A. C. Luntz, *ibid. 77* (1982) 3533, 3774.
[20] A. C. Luntz, R. Schinke, W. A. Lester, Jr., S. H. Günthard, *J. Chem. Phys. 70* (1979) 5908; A. C. Luntz, *ibid. 73* (1980) 1143, 5393.
[21] J. Franck, A. Eucken, *Z. Phys. Chem. Abt. B 20* (1933) 460.
[22] V. S. Letokhov, *Annu. Rev. Phys. Chem. 26* (1975) 133.
[23] M. Kneba, J. Wolfrum, *Annu. Rev. Phys. Chem. 31* (1980) 47.
[24] F. London, *Z. Elektrochem. Angew. Phys. Chem. 35* (1929) 552.
[25] P. Siegbahn, B. Liu, *J. Chem. Phys. 68* (1978) 2455; *80* (1984) 581.
[26] J. Wolfrum in W. Jost (Ed.): *Atom Reactions in Physical Chemistry - an Advanced Treatise*. Academic Press, New York 1975.
[27] U. Wellhausen, J. Wolfrum, *Ber. Bunsenges. Phys. Chem. 89* (1985) 314.
[28] J. Wolfrum, *J. Phys. Chem. 90* (1986) 375.
[29] T. Dreier, J. Wolfrum, *Int. J. Chem. Kinet. 18* (1986) 919.
[30] H. R. Mayne, J. P. Toennies, *J. Chem. Phys. 75* (1981) 1754.
[31] D. D. Gerrity, J. J. Valentini, *J. Chem. Phys. 79* (1983) 5202; C. T. Rettner, E. E. Marinero, R. N. Zare, *ibid. 80* (1984) 4142; R. Götting, H. R. Mayne, J. P. Toennies, *ibid. 80* (1984) 2230.
[32] M. Kneba, J. Wolfrum, *J. Phys. Chem. 83* (1979) 69.
[33] D. K. Bondi, J. N. L. Connor, J. Manz, J. Römelt, *Mol. Phys. 50* (1983) 467.
[34] D. Arnoldi, K. Kaufmann, J. Wolfrum, *Phys. Rev. Lett. 34* (1975) 1597.
[35] R. S. Sheorey, G. W. Flynn, *J. Chem. Phys. 72* (1980) 1175; M. Kneba, R. Stender, U. Wellhausen, J. Wolfrum, *J. Mol. Struct. 59* (1980) 207.
[36] H. Frei, G. C. Pimentel, *J. Phys. Chem. 85* (1981) 3355.
[37] H. Frei, G. C. Pimentel, *J. Chem. Phys. 78* (1983) 3698; A. Knudsen, G. C. Pimentel, *ibid. 78* (1983) 6780.
[38] P. Hering, P. R. Brooks, R. F. Curl, R. S. Judson, R. S. Lowe, *Phys. Rev. Lett. 44* (1980) 687; H. P. Grieneisen, J. Xue-Jing, K. L. Kompa, *Chem. Phys. Lett. 82* (1981) 421; C. Jouvet, B. Soep, *ibid. 96* (1983) 426.
[39] T. C. Maguire, P. R. Brooks, R. F. Curl, Jr., *Phys. Rev. Lett. 50* (1983) 1918.
[40] P. Arrowsmith, P. E. Bartoszek, S. H. P. Bly, T. Carrington, P. E. Charters, J. C. Polanyi, *J. Chem. Phys. 73* (1980) 5895; P. Arrowsmith, S. H. P. Bly, P. E. Charters, J. C. Polanyi, *ibid. 79* (1983) 283.
[41] D. G. Imre, J. L. Kinsey, R. W. Field, D. H. Katayama, *J. Phys. Chem. 86* (1982) 2564.
[42] D. G. Imre, J. L. Kinsey, A. Sinha, J. Krenos, *J. Phys. Chem. 88* (1984) 3956.
[43] R. C. Estler, R. N. Zare, *J. Am. Chem. Soc. 100* (1978) 1323.
[44] G. G. Balint-Kurti, R. N. Yardley, *Faraday Discuss. Chem. Soc. 62* (1977) 77.
[45] C. T. Rettner, R. N. Zare, *J. Chem. Phys. 75* (1981) 3636.
[46] D. Astholz, J. Troe, W. Wieters, *J. Chem. Phys. 70* (1979) 5107.
[47] J. Troe, W. Wieters, *J. Chem. Phys. 71* (1979) 3931.
[48] H. Hippler, J. Troe, H. J. Wendelken, *J. Chem. Phys. 78* (1983) 6709; H. Hippler, K. Luther, J. Troe, H. J. Wendelken, *ibid. 79* (1983) 239.
[49] D. J. Perettie, J. C. Stevens, J. B. Clark, *NATO ASI Ser. Ser. B 105* (1984) 239.
[50] S. W. Benson, US-Pat. 4 199 533 (1980).
[51] K. V. Reddy, *Proc. SPIE Int. Soc. Opt. Eng. 458* (1984) 53.
[52] A. Kaldor, *NATO Adv. Study Inst.* (San Miniato, Italy 1982) lecture.
[53] D. J. Perettie, *NATO Adv. Study Inst.* (San Miniato, Italy 1982) lecture.
[54] R. G. Bray, M. S. Chou, *Proc. SPIE Int. Soc. Opt. Eng. 458* (1984) 75.
[55] Zhang Yunwu, W. Fuß, K. L. Kompa, F. Rebentrost, *Laser Chem. 5* (1985) 257.
[56] P. Ehrlich, R. N. Pittilo, *Hochpol. Forsch. 7* (1970) 386; G. Luft, *CZ Chem. Tech. 2* (1973) 89; M. Buback, H. Lendle, *Makromol. Chem. 184* (1983) 193; M. Buback, H. Hippler, J. Schweer, H. P. Vögele, *Makromol. Chem. Rapid Commun. 7* (1986) 261; H. Brademann, M. Buback, H. P. Vögele, *Makromol. Chem. 187* (1986) 1977.
[57] S. G. Il'Yasov, I. N. Kalvina, G. A. Kyulyan, V. F. Moskalenko, E. P. Ostapchenko, *Sov. J. Quantum Electron. (Engl. Transl.) 4* (1975) 1287; J. P. Fouassier, P. Jaques, D. J. Lougnot, T. Pilot, *Polym. Photochem. 5* (1984) 57.
[58] R. K. Sadhir, J. D. B. Smith, P. M. Castle, *J. Polym. Sci. Polym. Chem. Ed. 23* (1985) 411.
[59] C. Decker, *J. Polym. Sci. Polym. Chem. Ed. 21* (1983) 2451.
[60] S. P. Pappas, B. C. Pappas, L. R. Gatechair, W. Schnabel, *J. Polym. Sci. Polym. Chem. Ed. 22* (1984) 69.
[61] R. Bussas, K. L. Kompa in *Max-Planck Inst. Quantenopt. (Ber.) 1984.*
[62] G. Amirzadeh, W. Schnabel, *Makromol. Chem. 182* (1981) 2821; T. Sumiyoski, W. Weber, W. Schnabel, *Z. Naturforsch. A 40* (1985) 541; C. E. Hoyle, R. D. Hensel, M. B. Grubb, *J. Polym. Sci. Polym. Chem. Ed. 22* (1984) 1865.
[63] D. J. Ehrlich, J. Y. Tsao, *Appl. Phys. Lett. 46* (1985) 198.
[64] H. Niederwald, K. H. Richter, W. Güttler, M. Schwörer, *Mol. Cryst. Liq. Cryst. 93* (1983) 247.
[65] C. Bräuchle, D. M. Burland, *Angew. Chem. 95* (1983) 612; *Angew. Chem. Int. Ed. Engl. 22* (1983) 582.
[66] G. L. Paul, *Conf. Lasers Electroopt.* (San Francisco 1986) p. 48.
[67] R. E. Schwerzel, V. E. Wood, V. D. McGiuniss, C. M. Verber, *Proc. SPIE Int. Soc. Opt. Eng. 458* (1984) 90; F. Nakai, Y. Marutani, *Conf. Lasers Electroopt.* (San Francisco 1986) p. 42.
[68] M. Fischer, *Angew. Chem. 90* (1978) 17; *Angew. Chem. Int. Ed. Engl. 17* (1978) 16.
[69] V. Malatesta, C. Willis, P. A. Hackett, *J. Am. Chem. Soc. 103* (1981) 6781.
[70] W. G. Dauben, R. B. Phillips, *J. Am. Chem. Soc. 104* (1982) 858.
[71] N. Gottfried, W. Kaiser, M. Braun, W. Fuss, K. L. Kompa, *Chem. Phys. Lett. 110* (1984) 335.
[72] P. A. Hackett, C. Willis, M. Gauthier, A. J. Alcock, *Proc. SPIE Int. Soc. Opt. Eng. 458* (1984) 65.
[73] R. M. Wilson in A. Padwa (Ed.): *Organic Photochemistry, Vol. 7*. Dekker, New York 1985, Chap. 5; *Proc. SPIE Int. Soc. Opt. Eng. 458* (1984) 58.
[74] W. Adam, K. Hannemann, R. M. Wilson, *J. Am. Chem. Soc. 108* (1986) 929; see also W. Adam, M. Dörr, P. Hössel, *Angew. Chem. 98* (1986) 820; *Angew. Chem. Int. Ed. Engl. 25* (1986) 818.
[75] D. H. R. Barton, B. Chapiot, K. U. Ingold, L. J. Johnston, W. B. Motherwell, J. C. Scaniano, S. Stanforth, *J. Am. Chem. Soc. 107* (1985) 3607; N. Bischofberger, B. Frei, J. Wirz, *Helv. Chim. Acta 66* (1983) 2485; E. F. Hilinski, D. Huppert, D. F. Kelley, S. V. Milton, P. M. Rentzepis, *J. Am. Chem. Soc. 106* (1984) 1951; C. V. Kumar, D. Ramaiah, P. K. Das, M. V. George, *J. Org. Chem. 50* (1985) 2818.
[76] V. S. Letokhov in H. Grünewald (Ed.): *Chemistry for the Future*. Pergamon, New York 1984, p. 253.
[77] U. Brackmann, F. P. Schäfer, *Chem. Phys. Lett. 87* (1982) 579.
[78] V. S. Letokhov, Y. A. Matveetz, V. A. Semchishen, E. V. Khoroshilova, *Appl. Phys. B 36* (1985) 243.
[79] D. N. Nikogosyan, *VII. USSR-BRD Laser Spectrosc. Semin.* (Baku, UdSSR 1985).
[80] W. Kuhn, E. Knopf, *Z. Phys. Chem. Abt. B 7* (1930) 292.
[81] L. A. Rebane, A. A. Gorokhovskii, J. V. Kikas, *Appl. Phys. B 29* (1982) 235; M. Eich, J. H. Wendorff, H. Ringsdorf, H. W. Schmidt, *Makromol. Chem. 186* (1985) 2639.
[82] J. Friedrich, D. Haarer, *Angew. Chem. 96* (1984) 96; *Angew. Chem. Int. Ed. Engl. 23* (1984) 113.
[83] A. Winnacker, R. M. Shelby, R. M. Macfarlane, *Opt. Lett. 10* (1985) 350.
[84] H. W. H. Lee, M. Gehrtz, E. E. Marinero, W. F. Moerner, *Chem. Phys. Lett. 118* (1985) 611.
[85] W. Kuhn, H. Martin, *Z. Phys. Chem. Abt. B 21* (1933) 93; C. B. Moore (Ed.): *Chemical and Biochemical Applications of Laser*. Academic Press, New York 1977.
[86] F. S. Becker, K. L. Kompa, *Nucl. Technol. 58* (1982) 329.
[87] J. I. Davis, J. Z. Holtz, M. L. Spaeth, *Laser Focus Fiberopt. Technol. 18* (1982) 49; *Conf. Lasers Electroopt.* (San Francisco 1986) p. 89.
[88] R. W. Solarz, GRA *85* (1985) 24; R. L. Byer, *IEEE J. Quantum Electron. QE 12* (1976) 732.
[89] P. Rabinowitz, A. Stein, R. Brickman, A. Kaldor, *Appl. Phys. Lett. 35* (1979) 793.
[90] K. C. Kim, S. M. Freund, M. S. Sorem, D. F. Smith, *J. Chem. Phys. 83* (1985) 4344.
[91] H. J. Circel in W. Waidelich (Ed.): *Optoelectronics in Engineering*. Springer, Heidelberg 1986, p. 706.
[92] S. S. Miller, D. D. DeFord, T. J. Marks, E. Weitz, *J. Am. Chem. Soc. 101* (1979) 1036.
[93] A. Kaldor, R. L. Woodin, *Proc. IEEE 70* (1982) 565.
[94] R. Cunningham, *Lasers and Applications 4* (1985) 11.
[95] M. R. Humphries, O. L. Boarne, P. A. Hackett, *Chem. Phys. Lett. 118* (1985) 134; A. V. Evseev, V. S. Letokhov, A. A. Puretzky, *Appl. Phys. B 36* (1985) 93.
[96] Zhang Linyang, Zhang Yunwu, Ma Xingxiao, Yuan Peng, Xu Yan, Gong Mengxiong, W. Fuß, *Appl. Phys. B 39* (1986) 117.
[97] F. Magnotta, I. P. Herman, *J. Chem. Phys. 81* (1984) 2363.
[98] K. Takendu, S. Satooka, Y. Makide, *Appl. Phys. B 33* (1984) 83; F. Magnotta, I. P. Herman, *ibid. 36* (1985) 207.
[99] J. H. Clark, Y. Haas, P. L. Houston, C. B. Moore, *Chem. Phys. Lett. 35* (1975) 82; R. E. M. Hedges, P. Ho, C. B. Moore, *Appl. Phys. B 23* (1980) 25; L. Mannik, S. K. Brown, *ibid. 37* (1985) 75.
[100] A. Outhouse, P. Lawrence, M. Gauthier, P. A. Hackett, *Appl. Phys. B 36* (1985) 63; R. J. Nadalin, R. G. Charles, U.S. Pat. 4496495 (1985), Westinghouse Electric Corp.
[101] J. Moser, P. Morand, R. Duperrex, H. van den Bergh, *Chem. Phys. 79* (1983) 277.
[102] W. Fuss, W. E. Schmidt, K. L. Kompa, *Verh. Dtsch. Phys. Ges. 20* (1985) 1056.

[103] O. N. Avatkov, A. B. Bakhtadze, V. Yu. Baranov, V. S. Doljikov, I. G. Gverdsiteli, S. A. Kazakov, V. S. Letokhov, V. D. Pismmenyi, E. A. Ryobov, V. M. Vetsko, *Appl. Opt. 23* (1984) 26.
[104] T. J. Manuccia, M. D. Clark, E. R. Lory, *J. Chem. Phys. 68* (1978) 227.
[105] M. Stuke, *Spektrum Wiss. 1982*, No. 4, p. 76.
[106] J. H. Clark, R. G. Anderson, *Appl. Phys. Lett. 32* (1978) 46; A. Hartford, *J. Appl. Phys. 51* (1980) 4471.
[107] J. A. Merritt, L. C. Robertson, *J. Chem. Phys. 67* (1977) 3545.
[108] R. V. Ambartzumyan, *Sov. J. Quantum Electron. (Engl. Transl.) 6* (1977) 96.
[109] E. M. Geiser, R. W. Johnson, U.S. Pat. 4287038 (1981).
[110] T. Donohue, *J. Chem. Phys. 67* (1977) 5402; *Conf. Lasers Electroopt.* (Phoenix, AZ, 1982) p. 95.
[111] H. L. Chen, C. Borzileri, *IEEE J. Quantum Electron. QE 16* (1980) 1229.
[112] A. Gupta, J. T. Yardley, *Proc. SPIE Int. Soc. Opt. Eng. 458* (1984) 131.
[113] W. M. Shaub, S. H. Bauer, *Int. J. Chem. Kinet. 7* (1975) 509.
[114] D. J. Frurip, P. R. Staszak, M. Blander, *J. Non-Cryst. Solids 68* (1984) 1.
[115] Y. Kizaki, T. Kandori, Y. Fujitani, *Jpn. J. Appl. Phys. 24* (1985) 806.
[116] G. W. Rice, R. L. Woodin, *Proc. SPIE Int. Soc. Opt. Eng. 458* (1984) 98.
[117] W. R. Cannon, S. C. Danforth, J. H. Flint, J. S. Haggerty, R. A. Marra, *J. Am. Ceram. Soc. 65* (1982) 324; W. R. Cannon, S. C. Danforth, J. S. Haggerty, R. A. Marra, *ibid. 65* (1982) 330; J. H. Flint, J. S. Haggerty, *Proc. SPIE Int. Soc. Opt. Eng. 458* (1984) 108.
[118] J. C. Mitchener, M. S. Wrighton, *J. Am. Chem. Soc. 103* (1981) 975.
[119] R. L. Whetten, K. J. Fu, E. R. Grant, *J. Am. Chem. Soc. 104* (1982) 4270.
[120] D. J. Perettie, M. S. Paquette, R. L. Yates, H. D. Gafne, *NATO ASI Ser. Ser. B 105* (1984) 259.
[121] E. Huber, M. von Allmen, *Phys. Rev. B Condens. Matter 28* (1983) 2979; M. von Allmen, *Mater. Res. Soc. Symp. Proc. 13* (1983) 691; K. Attolter, M. von Allmen, *Appl. Phys. A 33* (1984) 93.
[122] S. D. Allen, *J. Appl. Phys. 52* (1981) 6501; D. Bäuerle, P. Irsingler, G. Leyendecker, H. Noll, D. Wagner, *Appl. Phys. Lett. 40* (1982) 819.
[123] G. D. Davis, C. A. Moore, R. A. Goltscho, *J. Appl. Phys. 56* (1984) 1808.
[124] R. Solanki, W. H. Ritchie, G. J. Collins, *Appl. Phys. Lett. 43* (1983) 454.
[125] T. F. Deutsch, D. J. Ehrlich, R. M. Osgood, *Appl. Phys. Lett. 35* (1979) 381.
[126] D. J. Ehrlich, R. M. Osgood, T. F. Deutsch, *J. Vac. Sci. Technol. 21* (1982) 23.
[127] W. Kräuter, D. Bäuerle, F. Fimberger, *Appl. Phys. A 31* (1983) 13.
[128] D. J. Ehrlich, J. Y. Tsao, *J. Vac. Sci. Technol. B 1* (1983) 969; D. J. Ehrlich, J. Y. Tsao, *Springer Ser. Chem. Phys. 39* (1984) 386.
[129] R. Bilinchi, I. Gianinoni, M. Musci, R. Murri, S. Tacchetti, *Appl. Phys. Lett. 47* (1985) 279; H. M. Branz, S. Fan, J. H. Flint, D. Adler, J. S. Haggerty, *ibid. 48* (1986) 171.
[130] H. Schröder, K. L. Kompa, D. Musci, I. Gianinoni, *Appl. Phys. A 38* (1985) 227.
[131] W. G. Hollingsworth, V. Vaida, *J. Phys. Chem. 90* (1986) 1235.
[132] R. Fantoni, M. Stuke, *Appl. Phys. B 38* (1985) 209; *Verh. Dtsch. Phys. Ges. 21* (1986) 657.
[133] R. J. von Gutfeld, E. E. Tynan, R. L. Melcher, S. E. Blum, *Appl. Phys. Lett. 35* (1979) 651.
[134] H. Pummer, *Phys. Bl. 41* (1985) 199.
[135] R. Srinivasan: *Photophysics and Photochemistry above 6 eV*, Elsevier, Amsterdam 1985, p. 595; G. Gorodetsky, T. G. Kazyaka, R. L. Melcher, R. Srinivasan, *Appl. Phys. Lett. 46* (1985) 828.
[136] F. Friedrich, Ch. J. Raub, *Metalloberfläche 38* (1984) 237; R. J. von Gutfeld, D. R. Vigliotti, *Appl. Phys. Lett. 46* (1985) 1003.
[137] G. J. Müller, P. Berlien, C. Scholz, *Umschau (1982) 86* (1986) 233.
[138] A. Anders, *Proc. SPIE Int. Soc. Opt. Eng. 236* (1980) 160; V. S. Letokhov, *Nature (London) 316* (1985) 327.
[139] T. I. Karu, G. S. Kalendo, V. S. Letokhov, V. V. Lobko, *Sov. J. Quantum Electron. (Engl. transl.) 13* (1983) 1169.
[140] J. M. Isner, R. H. Clarke, *IEEE J. Quantum Electron. QE 20* (1984) 1406; R. Thull, *Herz und Gefäße 5* (1985) 179.
[141] G. S. Abela, S. Normann, D. Cohen, R. L. Feldmann, E. A. Geiser, C. R. Conti, *Am. J. Cardiol. 50* (1982) 1199; D. S. J. Choi, S. Stertzer, H. Rotterdam, M. S. Burns, *ibid. 50* (1982) 1209.
[142] D. Muller, *Lasers and Applications 5* (1986) 85.
[143] F. W. Mohr, K. O. Greulich, R. Weller, J. Wolfrum, W. Lenz, S. V. Kuserow, P. G. Kirchhoff, *3. Jahrestag. Dtsch. Ges. Lasermedizin*. Lübeck-Travemünde 1986.
[144] E. M. H. Mathus-Vliegen, G. N. J. Tytgat, *Cancer (Philadelphia) 57* (1986) 396.
[145] J. C. van Gemert, M. C. Berenbaum, G. H. M. Gijsers, *Br. J. Cancer 52* (1985) 43.
[146] J. S. Nelson, W. H. Wright, M. W. Berns, *Cancer Res. 45* (1985) 5781.
[147] D. A. Bellnier, C. W. Lin, G. R. Prout, Jr., *JNCI J. Natl. Cancer Inst.*, in press.
[148] R. Hilf, R. S. Murant, U. Narayanan, S. L. Gibson, *Cancer Res. 46* (1986) 211.
[149] G. S. Lin, A. A. Al Dakan, D. P. Gibson, *Br. J. Cancer 53* (1986) 265.
[150] L. Herrera-Ornelas, N. J. Petrelli, A. Mittelman, T. J. Dougherty, D. B. Boyles, *Cancer (Philadelphia) 57* (1986) 677.
[151] M. Moretti, *Lasers and Applications 4* (1985) 46.
[152] O. J. Beck, F. Frank, E. Keiditsch, F. Wondrazek, *Laser 1* (1985) 13.
[153] R. Schober, F. Ulrich, T. Saner, H. Dürselen, S. Hessel, *Science (Washington) 232* (1986) 1421.
[154] D. Katalinic, *Laser 1* (1985) 57.
[155] J. Kaplan, S. Giler (Eds.): *CO_2 Laser Surgery*, Springer, Berlin 1984.
[156] C. A. Puliafito, R. F. Steinert, *Laser Focus (Littleton Mass.) 1985*, September issue p. 84.
[157] C. A. Puliafito, R. F. Steinert, *IEEE J. Quantum Electron QE 20* (1984) 1442.
[158] J. Marshall, S. Trokel, S. Rothery, R. R. Krueger, *Lasers Ophthalmol. 1* (1986) 1; R. Scinivasan, *Science 234* (1986) 559.
[159] U. Klingbeil, A. Plesch, J. Bille, O. Käfer, *Fortschr. Ophthalmol. 79* (1982) 275.
[160] J. Troe, *J. Phys. Chem. 90* (1986) 357.
[161] W. Kaiser, *Phys. Bl. 41* (1985) 370.